

# SIR epidemiological model with ratio-dependent incidence: influence of preventive vaccination and treatment control strategies on disease dynamics

Udai Kumar<sup>a</sup>, Partha Sarathi Mandal<sup>a\*</sup>, Jai Prakash Tripathi<sup>b</sup>, Vijay Pal Bajiyya<sup>b</sup>, Sarita Bugalia<sup>b</sup>

<sup>a</sup>Department of Mathematics, NIT Patna  
Patna-800005, Bihar, India

<sup>b</sup>Department of Mathematics, Central University of Rajasthan  
Kishangarh 305817, Ajmer, Rajasthan, India

## Abstract

In this paper, we study a SIR epidemic model with ratio dependent incident rate function describing the mechanisms of infectious disease transmission. The proposed model system explore the impact of vaccination and treatment on the transmission dynamics of the disease. The treatment control strategies depend on the availability of maximal treatment capacity: the treatment rate is constant when the number of infected individuals is greater than the maximal capacity of treatment and proportional to the number of infected individuals when the number of infected individuals is less than the maximal capacity of treatment. The existence and stability of the endemic equilibria are governed by the basic reproduction number and treatment control strategies. By carrying out rigorous mathematical analysis combined with numerical simulations of the proposed model system, it has been shown that (1) the sufficiently large value of the preventive vaccination rate can control the spread of disease, (2) a threshold level of the psychological (or inhibitory) effects in the incidence rate function is enough to decrease the infective population. It is also obtained that model system undergoes a transcritical and a saddle-node bifurcations with respect to disease contact rate. Moreover, in the presence of treatment strategies, the model system have multiple endemic equilibria and undergoes a backward bifurcation. The maximal capacity of treatment plays important roles on the disease dynamics of the model system. The number of infected individuals decreases with respect to the maximal capacity of treatment and the disease completely dies out from the system for the large capacity of the treatment when constant treatment strategy is applied. Further, it is also found that the spread of disease can be suppressed by increasing treatment rate. From sensitivity analysis, we have observed that the transmission and treatment rates are most sensitive parameters on the model system. Moreover, the effects of different parameters on the disease dynamics have also been investigated via numerical simulation.

**Keywords:** SIR model; Nonlinear incidence; Stability; Treatment strategies; Backward bifurcations; Multiple endemic equilibria.

---

\*Corresponding author, E-mail: partha.000@gmail.com

# 1 Introduction

Diseases (communicable and non-communicable) are the big problems of human health and they have become one of most common causes for death. In a press release in 1996, WHO claims that out of 52 million death in 1995, more than 17 million were due to infectious diseases [1]. On one side, the mathematical models for the spread of infectious diseases help us to predict likely behaviours of future outbreaks and to demonstrate past outbreaks, on the other side, it also make us able to predict the effect of mitigating and intervention strategies. The model formulation process clarifies assumptions, variables, and parameters; moreover, models provide conceptual results such as thresholds, basic reproduction numbers, contact numbers, and replacement numbers [4, 5, 10]. Mathematical models and computer simulations are useful experimental tools for building and testing theories, assessing quantitative conjectures, answering specific questions, determining sensitivities to changes in parameter values, and estimating key parameters from data. Better understanding of the transmission characteristics of a particular infectious disease in a community/country can lead to better approaches to reduce/control the transmission of the disease. For comparing, planning, implementing, evaluating, and optimizing various detection, prevention, therapy, and control programs, mathematical models have been playing valuable role [4, 14, 26, 27, 42]. Thus, suitable mathematical models provide proper suggestions/information which help to improve preparedness and response against infectious disease.

A very fruitful modeling paradigm in epidemiology is the so-called compartmental models. Several compartmental models for the spread of infectious diseases in populations have been analyzed mathematically and applied to specific diseases [4, 5, 20]. The rate of new infections (incidence rate) plays a crucial role in modeling of infectious diseases [6, 12]. In most of the epidemic models (Anderson and May [4]), the incidence rate (the number of new cases per unit time) takes the mass-action form with bilinear interactions. However, several authors [2, 6, 7, 12, 17, 21, 32] have suggested for non-linear incidence rate in disease transmission progress. In particular, incidence rate function  $g(I)S$  describes the mechanism of disease transmission i.e., rate at which susceptible become infectious [3, 28]. Density of population, life style and media coverage may affect the incidence rate function directly or indirectly [14]. There are many reasons for using nonlinear incidence rates, for example, psychological effects: for a very large number of infectives the infection force may decrease as the number of infective individuals increases, because in the presence of large number of infectives the population may tend to reduce the number of contacts per unit time [8]; crowding of infective individuals or due to the protection

measures by the susceptible individuals [8]; intervention policies: when infected individuals are large enough, we perform intervention policies, for example, closing schools, restaurants and postponing conferences [15].

The general non-linear incidence rate used by Liu et al. [18, 19] to incorporate the effect of the behavioral changes of the susceptible individuals is of the following form:

$$g(I)S = \frac{kI^l}{1 + \alpha I^h} S, \quad (1)$$

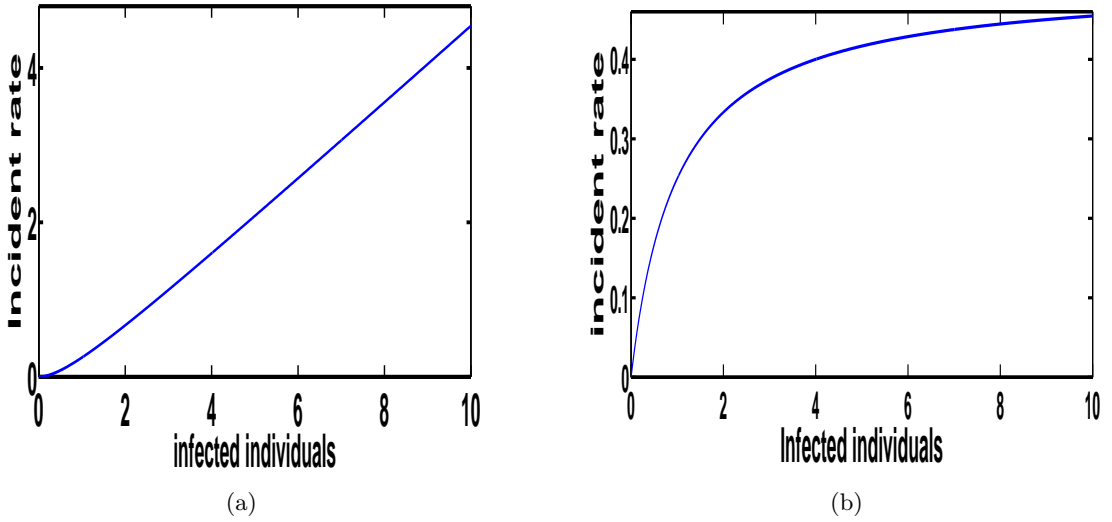


Figure 1: Figure depicts per capita incident rate for different value of l and h. (a) Unbounded incidence rate function (l=2, h=1). (b) Saturated incidence rate function (l=1, h=1)

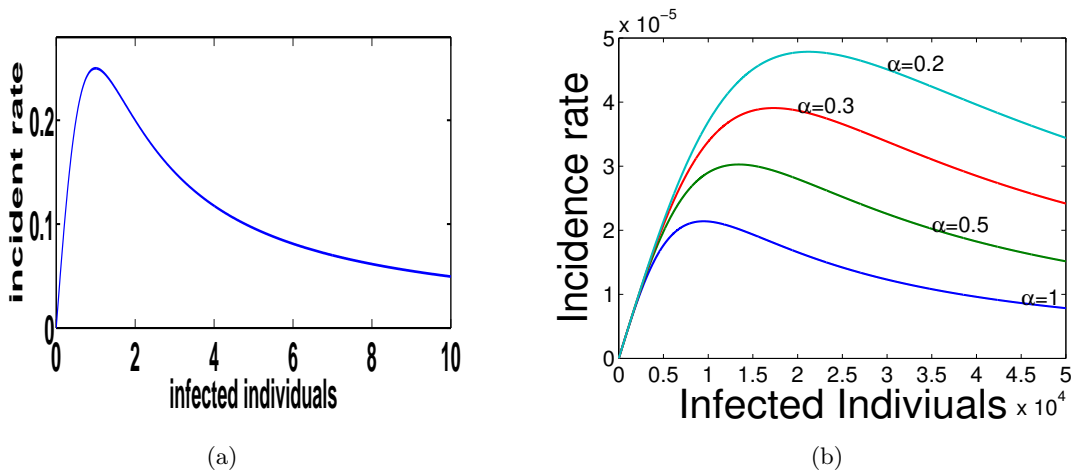


Figure 2: Figure illustrates per capita incident rate and effect of human behavior on per capita incidence rate. (a) Non-monotonic incidence rate function (l = 1, h = 2). (b) Effect of human behavior (l = 1, h = 2). It shows how  $\alpha$  (parameter measuring the psychological/inhibitory effect) impacts per capita incidence rate.

where the parameters  $l$  and  $h$  are positive constants;  $k$  is the probability of transmission *per* contact *per* unit time;  $\alpha$  is non negative constant which measures the psychological or inhibitory effects;  $kI^l$  measures the infection force of the disease and  $\frac{1}{1+\alpha I^h}$  measures the inhibition effect from the behavioral change of the susceptible individuals when their number increases (or from the crowding effect of the infective individuals). Psychological effect influences the incidence rate function. For a very large number of infectives, the infection force may decrease as the number of infective individuals increases because the population may tend to reduce the number of contacts per unit time in the presence of large number of infectives [8, 33]. In fact, when a new infectious disease occurs, both the infection and the contact rate probability increase since people have less knowledge about the disease. However, when the number of infected individuals increases and the disease becomes more serious, psychological factor leads people to improve their behavior ((e.g., to avoid shaking hands, frequent washing of hands, closure of schools and offices, less mobility etc.)) and adopt suitable measures to reduce the possibility of contact and infection probability. Many authors, for instance, Hethcote [3], Xiao and Ruan [33], Derrick and van den Driessche [34], Hethcote and Levin [35], van den Driessche [36], Ruan and Wang [8], Alexander and Moghadas [42], Tang et al. [13] and so forth have used specific values for  $l$ ,  $h$ . The nonlinear incidence function given in (1) could be derived in the following three different forms:

1. In many standard epidemic models [9, 24, 26, 42, 43] bilinear incidence rate have been expressed as  $kS(t)I(t)$  where  $S(t)$  and  $I(t)$  are the susceptible and infective individual at time  $t$ , respectively and  $k$  is the disease contact parameter. For  $l > h$ , the incidence function is unbounded (cf. Figure 1 (a)). Dynamics of epidemic models with unbounded incidence rates are similar to those with bilinear incidence rates. Hethcote and van den Driessche [36] considered bilinear incidence rate by taking  $l = h + 1$ .
2. The incidence function may tend to a saturation level as the number of infectious individuals becomes large enough [15, 22] (refer the Figure 1 (b)). This is very reasonable because the number of effective contacts between infective individuals and susceptible individuals may saturate at high infective levels due to crowding of infective individuals or due to the protection measures adopted by the susceptible individuals. Capasso and Serio [22] considered,  $l = h = 1$  in the saturated incidence function and therefore the incidence function given in (1) takes the form  $g(I) = \frac{kI}{1+\alpha I}$ . They described the dependency of infectives via nonlinear saturated bounded incidence function for large numbers of infectives. The authors studied the “crowding effect” or “protection measures” while modeling the cholera epidemics in Bari in 1973. The dynamics of epidemic models with saturated incidence

rates (when  $l = h$ ) have been shown to be very rich and complex. For a SEIRS model system with  $l = h$ , Hethcote and van den Driessche [36] observed that the threshold concept becomes more complicated since the asymptotic behavior depends on both thresholds and the initial values. The model system will have none, one, or two endemic equilibria, and the disease may die out beyond the threshold for some initial values. Further periodic solutions also appear through Hopf bifurcation. The results of [36] are analogous to those obtained by Liu, Hethcote, and Levin [18] for SIRS models with  $l = h$  (cf. Figure 1 (b)). The case  $l = h = 1$  has also been discussed briefly by Gomes et al. [23], who obtained the existence of backward bifurcation, oscillations, and Bogdanov–Takens bifurcation in SIR and SIS model systems.

3. Wang [15], Xiao and Ruan [33] introduced non-monotone incidence function by considering  $l < h$  (cf. Figure 2 (a)). Xiao and Ruan [33] described the psychological effect of certain serious diseases (for instance, *SARS* and some sexually-transmitted-diseases) on the community when the number of infectives become larger. They have also described the global analysis of the model and studied the stability of the disease-free and the endemic equilibrium. Further authors concluded that either the number of infective individuals tends to zero as time evolves or the disease persists.

The Figure 2(b) shows that if we increase the value of  $\alpha$ , then the incidence rate saturates at lower value and also peak point of incidence rate decreases. Thus the incidence rate decrease with increase in infection cases due to effects of behavioral changes in susceptible population. Thus one can say that Fig. 2(b) shows that if the number of infected individuals increases then susceptible individuals start avoiding to contact with infectious individuals (e.g., to avoid shaking hands, frequent washing of hands, closure of schools etc.) The infection force ( $g(I)$ ) in Eq. (1) is function of infective individuals only. However Yuan and Li [37] introduced the transmission of communicable diseases involving both infective and susceptible individuals. Infection force ought to depend on the densities of both infective and susceptible individuals and it should take the form  $g(I, S)$ . Further, Yuan and Li [37] proposed that the infection force is a function of ratio of the number of the infectives to that of the susceptible and infection force function takes the following form:

$$g(I, S) = g\left(\frac{I}{S}\right) = \frac{k(I/S)^l}{1 + \alpha(I/S)^h}. \quad (2)$$

The infectious disease can be removed by using sanitation, antibiotics, and vaccination. In general, for controlling/preventing the spread of diseases, two types of effective methods namely

quarantine [38, 39] and vaccination [11, 40, 62] are used. In particular, in the disease dynamic model systems, vaccination are used to reduce both the morbidity and mortality of individuals [11, 41, 42]. Further many researchers (see, for example, [29–31, 46, 53–55, 59]) have also introduced the importance of treatment in disease dynamic models. Treatment is an important method to reduce the spread of diseases such as *measles*, *tuberculosis* and *flu* [16, 44, 45]. In classical epidemic models, the treatment rate of infected individuals is assumed to be either constant or proportional to the number of infected individuals [15, 30]. However, this assumption does not seem very reasonable, it may require a lot of resources for treatment. In general, a country/community should have a reasonable capacity for treatment. If it is too large, the country/community may pay unnecessary cost. If it is too small, the country/community may face the risk of the outbreak of a particular disease [29, 30, 46].

In particular, Wang and Ruan [30] considered an SIR epidemic model with constant treatment rate. The model system exhibits various types of bifurcations under this treatment strategy. Zhou and Fan [52] considered Holling type II treatment function given by  $T(I) = \frac{\beta I}{1+\gamma I}$ ,  $\beta > 0$ ,  $\gamma > 0$ . The model system exhibits backward bifurcation and Hopf bifurcation with varying treatment resources and its supply efficiency. De Pincho et al. [62] studied the normalized version of SIMR model system with medical treatment. In this study, the authors applied the Hamiltonian Jacobi approach and discussed how minimum time function varies with respect to perturbations of initial conditions. Li and Cui [47] introduced SIRS model with nonlinear incidence rate and constant treatment. In [29], Wang explored the following treatment function:

$$T(I) = \begin{cases} rI, & \text{if } 0 \leq I \leq I_c, \\ K, & \text{if } I > I_c. \end{cases} \quad (3)$$

In expression (3), two types of treatment strategies are considered depending on infected population size. First, if infected population size is less than the maximum capacity of treatment ( $I_c$ ) then proportional treatment is incorporated. Second, if number of the infectives is greater than the maximal capacity  $I_c$  then constant treatment is provided. This explains the situation where the number of hospital beds are limited and patients have to be hospitalized.

In the mathematical model systems referenced above, in general, authors assumed that space is homogeneous and investigations are confined to a population. However, infectious diseases spread geographically over time. In addition, in previous studies, the authors have generally focused on the dynamics of compartmental model systems with a specific type of treatment function and incidence rate. However, investigating the disease dynamics of an epidemic model system with nonlinear incidence rate (ratio dependent incidence rate) in the presence of different

treatment functions may provide different useful informations via mathematical and numerical evaluations.

More importantly, we would be able to compare the model predictions in different cases. Therefore, the detailed evolution of SIR model system with different incidence rates and treatment functions, makes us curious about the dynamical characteristics of SIR model system with ratio dependent incidence rate in the presence of different treatment functions. In the presence of ratio dependent incident rate, we are intended to investigate the role of disease threshold i.e., basic reproduction number on the disease dynamic model system for two different treatment strategies. In the present study, another very important term is the maximal treatment capacity which cure the infectives to prevent the spread of disease. In the presence of ratio dependent incidence function, we are also interested to analyze the role of maximal treatment capacity for both the treatment strategies.

In the present study, we consider an SIR epidemic model system with ratio dependent incidence rate and two different treatment rates (i)  $T(I) = rI$ , if  $0 \leq I \leq I_c$  where  $r > 0$  is a proportionality constant and  $I_c$  is some fixed value, and (ii)  $T(I) = K$ , where  $K$  is the maximal capacity of treatment. The question that we want to pose here is the following: (i) How the ratio dependent incidence rate and maximum capacity of treatment along with the above two different treatment strategies affect the disease dynamics? Thus in the present work, our objectives are two fold: (i) to observe that how the endemic coexistence is governed under the influence of basic reproduction number in two different treatment strategies. (ii) to investigate how does the ratio dependent incidence rate perturb the previously obtained results.

In epidemiology, the concept of threshold i.e., basic reproduction number is very important in the spread/control of the spread of disease. Here, we shall examine that what are the parameters with most sensitivity to the disease threshold. More precisely, we also quantify that which model parameter is much responsible for endemic coexistence through sensitivity analysis of endemicity.

Rest of the paper is organized as follows. In the next Section, we introduce the mathematical model with ratio dependent incidence rate. Boundedness of solutions and basic reproduction number have also been derived. The existence of equilibria under different treatment functions are discussed in Section 3. Stability of equilibrium points along with some important remarks are given in Section 4. Bifurcation analysis is demonstrated in Section 5. In Section 6, we present the local and global sensitivity analysis. Section 7 is devoted to the numerical evaluations of the model system to validate theoretical findings. The paper ends with detailed discussion and future scope of the present study.

## 2 The model and boundedness

Let  $N(t)$  denotes the total population size at any time  $t$  which is divided into three subclasses-  $S(t)$  : the susceptible population,  $I(t)$  : the infected population, and  $R(t)$  : the recovered population. Here we consider the following two different treatment functions: (i)  $T(I) = rI$ , if  $0 \leq I \leq I_c$  where  $r > 0$  is a proportionality constant and  $I_c$  is some fixed value, and (ii)  $T(I) = K$ , where  $K$  is the maximal capacity of treatment. Further, we assume that the infection force is of the following form:

$$g(I, S) = \frac{kIS}{S^2 + \alpha I^2},$$

which is obtained by taking  $h = 2$  and  $l = 1$  in Eq. (2). We also consider that a fraction  $p$  of recruited individuals are vaccinated, where  $p \in (0, 1]$  and these individuals are moved in recovered class. Therefore, the dynamics of the SIR model with ratio-dependent incidence rate and treatment function ( $T(I)$ ) is governed by the following system of nonlinear ordinary differential equations:

$$\begin{aligned} \frac{dS}{dt} &= (1-p)b - dS - \frac{kIS^2}{S^2 + \alpha I^2} + \gamma R, \\ \frac{dI}{dt} &= \frac{kIS^2}{S^2 + \alpha I^2} - (d + \mu)I - T(I), \\ \frac{dR}{dt} &= pb + \mu I - (d + \gamma)R + T(I), \end{aligned} \quad (4)$$

whose state space is the first quadrant  $\mathbb{R}_+^3 = \{(S, I, R) : S \geq 0, I \geq 0, R \geq 0\}$ . The initial conditions are given by  $S(0) = S_0 \geq 0$ ,  $I(0) = I_0 \geq 0$ ,  $R(0) = R_0 \geq 0$ . The biological descriptions of parameters are given in Table 1.

Parameters	Biological description
$k$	disease contact rate
$\gamma$	rate at which recovered individuals lose immunity and return to the susceptible class
$\mu$	recovery rate of infective individuals
$p$	fraction of recruited individuals those are vaccinated
$d$	natural death rate of each population
$b$	recruitment rate of susceptible population
$r$	treatment rate
$K$	maximal capacity of treatment
$\alpha$	psychological or inhibitory effect

Table 1: Biological meaning of parameters for model system (4).

Further, the total population  $N(t) = S(t) + I(t) + R(t)$  and the growth rate of population at

time  $t$  satisfy the following equation

$$\frac{dN}{dt} = b - d(S + I + R) = b - dN,$$

which gives,  $N(t) \rightarrow \frac{b}{d}$  as  $t \rightarrow \infty$ . Therefore, the biological feasible region for the model system (4) is given by

$$\Omega = \left\{ (S, I, R) : 0 \leq S, I, R, S + I + R \leq \frac{b}{d} \right\}, \quad (5)$$

which gives the following lemma:

**Lemma 2.1.** *The set  $\Omega$  defined in (5) is positively invariant for the model system (4).*

Basic reproduction number (basic reproductive rate) ( $\mathcal{R}_0$ ) is defined as the average number of secondary infections that occur when one infective is introduced into a completely susceptible host population [4, 5, 27]. In recent epidemiological modeling literatures, the basic reproduction number  $\mathcal{R}_0$  is often used as the threshold quantity that determines whether a disease can invade a population. It is really useful because it help us to determine whether or not an infectious disease can spread through a population. Following the same procedure as discussed in [5, 10], the basic reproduction number ( $\mathcal{R}_0$ ), for our proposed model system (4) can be evaluated as following:

$$\mathcal{R}_0 = \frac{k}{d + \mu + r}. \quad (6)$$

From expression (6), we observe that  $\mathcal{R}_0$  depends on parameters  $k$ ,  $d$ ,  $\mu$  and  $r$ . Moreover  $\mathcal{R}_0$  increases with the increasing disease contact rate  $k$ , and decreases with the increasing death rate  $d$ , recovery rate  $\mu$  and treatment rate  $r$ .

### 3 Existence of equilibria

In this section, we consider the model system (4) with the treatment rate (3) and investigate the existence of equilibrium points. Model system (4) always has a disease-free equilibrium  $E^0 = (S^0, I^0, R^0)$ , which can be obtained by putting  $I = 0$  in the following system of equations:

$$(1 - p)b - dS - \frac{kIS^2}{S^2 + \alpha I^2} + \gamma R = 0, \quad (7a)$$

$$\frac{kIS^2}{S^2 + \alpha I^2} - (d + \mu)I - T(I) = 0, \quad (7b)$$

$$pb + \mu I - (d + \gamma)R + T(I) = 0, \quad (7c)$$

which is given by

$$S^0 = \frac{b((1-p)d + \gamma)}{d(d + \gamma)}, \quad I^0 = 0, \quad R^0 = \frac{pb}{d + \gamma}. \quad (8)$$

Because of positiveness of model parameters and  $0 < p < 1$ , expression (8) indicates that the disease-free equilibrium ( $E^0$ ) of system (4) always exists. Therefore, the disease dies out at the equilibrium level given by Eq. (8).

Now, we compute the interior equilibrium points for the case  $T(I) = rI, 0 < I \leq I_c$ , which satisfy the following system of equations:

$$(1-p)b - dS - \frac{kIS^2}{S^2 + \alpha I^2} + \gamma R = 0, \quad (9a)$$

$$\frac{kIS^2}{S^2 + \alpha I^2} - (d + \mu)I - rI = 0, \quad (9b)$$

$$pb + \mu I - (d + \gamma)R + rI = 0. \quad (9c)$$

The discussion of interior equilibrium point(s) has been presented by the following theorem:

**Theorem 3.1.** *Model system (4) has no interior equilibrium point if  $\mathcal{R}_0 < 1$ . For  $\mathcal{R}_0 > 1$ , if  $\left(\frac{\mu+r+d+\gamma}{d+\gamma}\right) < \sqrt{\frac{\alpha}{\mathcal{R}_0-1}}$  and  $\left(\frac{\mu+r+d+\gamma}{d+\gamma}\right) > \sqrt{\frac{\alpha}{\mathcal{R}_0-1}}$ , then model system (4) generates unique interior equilibrium point (for both cases) which are given by  $E(S_1, I_1, R_1)$  and  $E(S_2, I_2, R_2)$ , respectively, such that*

$$\begin{aligned} S_1 &= \left( \frac{(1-p)b}{d} + \frac{pb\gamma}{d(d+\gamma)} \right) \left( 1 - \frac{\mu+r+d+\gamma}{d+\gamma} \frac{1}{\frac{\mu+r+d+\gamma}{d+\gamma} - \sqrt{\frac{\alpha}{\mathcal{R}_0-1}}} \right), \\ I_1 &= \frac{1}{\frac{\mu+r+d+\gamma}{d+\gamma} - \sqrt{\frac{\alpha}{\mathcal{R}_0-1}}} \left( \frac{(1-p)b}{d} + \frac{pb\gamma}{d(d+\gamma)} \right), \\ R_1 &= \frac{pb}{d+\gamma} + \frac{\mu+r}{d+\gamma} \frac{1}{\frac{\mu+r+d+\gamma}{d+\gamma} - \sqrt{\frac{\alpha}{\mathcal{R}_0-1}}} \left( \frac{(1-p)b}{d} + \frac{pb\gamma}{d(d+\gamma)} \right), \\ S_2 &= \left( \frac{(1-p)b}{d} + \frac{pb\gamma}{d(d+\gamma)} \right) \left( 1 - \frac{\mu+r+d+\gamma}{d+\gamma} \frac{1}{\frac{\mu+r+d+\gamma}{d+\gamma} + \sqrt{\frac{\alpha}{\mathcal{R}_0-1}}} \right), \\ I_2 &= \frac{1}{\frac{\mu+r+d+\gamma}{d+\gamma} + \sqrt{\frac{\alpha}{\mathcal{R}_0-1}}} \left( \frac{(1-p)b}{d} + \frac{pb\gamma}{d(d+\gamma)} \right), \\ R_2 &= \frac{pb}{d+\gamma} + \frac{\mu+r}{d+\gamma} \frac{1}{\frac{\mu+r+d+\gamma}{d+\gamma} + \sqrt{\frac{\alpha}{\mathcal{R}_0-1}}} \left( \frac{(1-p)b}{d} + \frac{pb\gamma}{d(d+\gamma)} \right). \end{aligned}$$

*Proof.* From Eq. (9c), we have

$$R = \frac{pb}{d+\gamma} + \frac{\mu+r}{d+\gamma} I. \quad (10)$$

Further, from Eqs. (9a) and (9b), we obtain

$$dS = (1-p)b + \gamma R - (d + \mu + r)I = 0. \quad (11)$$

Using (10) in Eq. 11, we find

$$S = \frac{(1-p)b}{d} + \frac{\gamma pb}{d(d+\gamma)} - \frac{d + \mu + r + \gamma}{d + \gamma} I > 0, \text{ if } \frac{(1-p)b}{d} + \frac{\gamma pb}{d(d+\gamma)} > \frac{d + \mu + r + \gamma}{d + \gamma} I. \quad (12)$$

From Eq. (9b), we have

$$S^2 = \frac{\alpha}{\mathcal{R}_0 - 1} I^2. \quad (13)$$

Using Eq. (13) in Eq. (12), we obtain the following quadratic equation in  $I$

$$\left( \left( \frac{\mu + r + d + \gamma}{d + \gamma} \right)^2 - \frac{\alpha}{(\mathcal{R}_0 - 1)} \right) I^2 - 2 \left( \frac{(1-p)b}{d} + \frac{pb\gamma}{d(d+\gamma)} \right) \left( \frac{\mu + r + d + \gamma}{d + \gamma} \right) I + \left( \frac{(1-p)b}{d} + \frac{pb\gamma}{d(d+\gamma)} \right)^2 = 0. \quad (14)$$

Expression for the roots of Eq. (14) is given by

$$I_1 = \frac{1}{\frac{\mu+r+d+\gamma}{d+\gamma} - \sqrt{\frac{\alpha}{\mathcal{R}_0-1}}} \left( \frac{(1-p)b}{d} + \frac{pb\gamma}{d(d+\gamma)} \right), \quad (15a)$$

$$I_2 = \frac{1}{\frac{\mu+r+d+\gamma}{d+\gamma} + \sqrt{\frac{\alpha}{\mathcal{R}_0-1}}} \left( \frac{(1-p)b}{d} + \frac{pb\gamma}{d(d+\gamma)} \right). \quad (15b)$$

Now, using (15a) in Eq. (12), S-coordinate of interior equilibrium point is given by

$$S_1 = \left( \frac{(1-p)b}{d} + \frac{pb\gamma}{d(d+\gamma)} \right) \left( 1 - \frac{\mu + r + d + \gamma}{d + \gamma} \frac{1}{\frac{\mu+r+d+\gamma}{d+\gamma} - \sqrt{\frac{\alpha}{\mathcal{R}_0-1}}} \right). \quad (16)$$

Using (15b) in Eq. (12), S-coordinate of interior equilibrium point is given by

$$S_2 = \left( \frac{(1-p)b}{d} + \frac{pb\gamma}{d(d+\gamma)} \right) \left( 1 - \frac{\mu + r + d + \gamma}{d + \gamma} \frac{1}{\frac{\mu+r+d+\gamma}{d+\gamma} + \sqrt{\frac{\alpha}{\mathcal{R}_0-1}}} \right). \quad (17)$$

Using (15a) in Eq. (10), we obtain

$$R_1 = \frac{pb}{d + \gamma} + \frac{\mu + r}{d + \gamma} \frac{1}{\frac{\mu+r+d+\gamma}{d+\gamma} - \sqrt{\frac{\alpha}{\mathcal{R}_0-1}}} \left( \frac{(1-p)b}{d} + \frac{pb\gamma}{d(d+\gamma)} \right). \quad (18)$$

Further using (15b) in Eq. (10), we obtain

$$R_2 = \frac{pb}{d + \gamma} + \frac{\mu + r}{d + \gamma} \frac{1}{\frac{\mu+r+d+\gamma}{d+\gamma} + \sqrt{\frac{\alpha}{\mathcal{R}_0-1}}} \left( \frac{(1-p)b}{d} + \frac{pb\gamma}{d(d+\gamma)} \right). \quad (19)$$

We derive the number of interior equilibrium point(s) with the help of Eqs. (15a) and (15b).

Eqs. (15a) and (15b) assure that the  $I^*$  does not acquire positive value for  $\mathcal{R}_0 < 1$  which results no interior equilibrium point. For  $\mathcal{R}_0 > 1$ , the number of interior equilibrium point(s) have been discussed as follows:

- (i) If  $\left(\frac{\mu+r+d+\gamma}{d+\gamma}\right) < \sqrt{\frac{\alpha}{\mathcal{R}_0-1}}$ , then (15a) takes negative value and positive value is taken by (15b). Under this parametric condition, both (16) and (17) are positive. Therefore, using (17) and (19), model system (4) generates unique interior equilibrium point  $E(S_2, I_2, R_2)$ .
- (ii) If  $\left(\frac{\mu+r+d+\gamma}{d+\gamma}\right) > \sqrt{\frac{\alpha}{\mathcal{R}_0-1}}$ , then (15a) and (15b) are positive. Under this parametric condition, (16) is negative. Therefore, using (17) and (19), model system (4) has unique interior equilibrium point  $E(S_1, I_1, R_1)$ .

□

Thus we observe that the model system (4) with  $T(I) = rI$ , changes its interior equilibrium point from zero to one, which suggests us to investigate the transcritical bifurcation. We will provide the threshold value and corresponding transversality condition in bifurcation section.

Now we discuss the equilibria of model system (4) with treatment function  $T(I) = K, I > I_c$ . The equilibrium points satisfy the following system of equations:

$$(1-p)b - dS - \frac{kIS^2}{S^2 + \alpha I^2} + \gamma R = 0, \quad (20a)$$

$$\frac{kIS^2}{S^2 + \alpha I^2} - (d + \mu)I - K = 0, \quad (20b)$$

$$pb + \mu I - (d + \gamma)R + K = 0. \quad (20c)$$

For interior equilibria  $E^*(S^*, I^*, R^*)$ , from equation (20c), we have

$$R^* = \frac{pb + K}{d + \gamma} + \frac{\mu}{d + \gamma} I^*. \quad (21)$$

From Eqs. (20a) and (20b), we have

$$S^* = \frac{1}{d} \left( (1-p)b + \gamma R^* - (d + \mu) I^* - K \right). \quad (22)$$

Using Eq. (21) in Eq. (22), we obtain

$$S^* = \frac{1}{d} \left( (1-p)b - K + \frac{\gamma(pb + K)}{d + \gamma} \right) - \left( \frac{d + \gamma + \mu}{d + \gamma} \right) I^*, \quad (23)$$

where  $K < (1-p)b + \frac{\gamma(pb+K)}{d+\gamma}$ , and  $I^* < \frac{\frac{1}{d} \left( (1-p)b - K + \frac{\gamma(pb+K)}{d+\gamma} \right)}{\left( \frac{d+\gamma+\mu}{d+\gamma} \right)}$ . Using (21) and (23) in (20a), we obtain following cubic equation in  $I^*$

$$f(I) \equiv A_0 I^3 + A_1 I^2 + A_2 I + A_3 = 0, \quad (24)$$

with coefficients

$$\begin{aligned}
A_0 &= \left(\frac{\mu + d + \gamma}{d + \gamma}\right)^2 (\mu + d + r) \left(\mathcal{R}_0 - \frac{d + \mu}{d + \mu + r}\right) - \alpha(d + \mu), \\
A_1 &= -\frac{2}{d(d + \gamma)} (b(1 - p)(d + \gamma) + \gamma pb - Kd) \frac{\mu + d + \gamma}{d + \gamma} (\mu + d + r) \left(\mathcal{R}_0 - \frac{d + \mu}{d + \mu + r}\right) \\
&\quad - K \left( \left(\frac{\mu + d + \gamma}{d + \gamma}\right)^2 + \alpha \right), \\
A_2 &= \frac{b(1 - p)(d + \gamma) + \gamma pb - Kd}{d(d + \gamma)} \left( \frac{b(1 - p)(d + \gamma) + \gamma pb - Kd}{d(d + \gamma)} (\mu + d + r) \left(\mathcal{R}_0 - \frac{d + \mu}{d + \mu + r}\right) \right. \\
&\quad \left. + 2K \frac{\mu + d + \gamma}{d + \gamma} \right), \quad A_3 = -K \left( \frac{b(1 - p)(d + \gamma) + \gamma pb - Kd}{d(d + \gamma)} \right)^2.
\end{aligned} \tag{25}$$

We describe all possible parametric conditions for the appearance of roots of Eq. (24) in the following theorem:

**Theorem 3.2.** (A): If  $\mathcal{R}_0 < \frac{d + \mu}{d + \mu + r}$  and  $\frac{b(1 - p)(d + \gamma) + \gamma pb}{d} < K$ , then model system (4) has no interior equilibrium point.

(B): If  $\mathcal{R}_0 > \frac{d + \mu}{d + \mu + r}$ , then

Case-1: Choose  $K < \frac{b(1 - p)(d + \gamma) + \gamma pb}{d}$ , then (i) if  $A_0 > 0$ , then Eq. (24) can exhibit three positive roots, (ii) if  $A_0 < 0$ , then Eq. (24) can exhibit two positive roots.

Case-2: Choose  $K > \frac{b(1 - p)(d + \gamma) + \gamma pb}{d}$ , then (a) For  $A_0 < 0$ , (1) Eq. (24) can exhibit two positive roots if, (i)  $A_1 > 0$  and  $A_2 < 0$ , (ii)  $A_1 < 0$  and  $A_2 > 0$ , (iii)  $A_1 > 0$  and  $A_2 > 0$ . (2) Eq. (24) has no positive root if  $A_1 < 0$  and  $A_2 < 0$ , (b) For  $A_0 > 0$ , (1) Eq. (24) can exhibit unique positive root if, (i)  $A_1 > 0$  and  $A_2 < 0$ , (ii)  $A_1 > 0$  and  $A_2 > 0$ , (iii)  $A_1 < 0$  and  $A_2 < 0$ . (2) Eq. (24) has three positive roots if  $A_1 < 0$  and  $A_2 > 0$ .

*Proof.* (A) We notice that the coefficients of cubic equation (24) do not alter its sign for  $\mathcal{R}_0 < \frac{d + \mu}{d + \mu + r}$  and  $\frac{b(1 - p)(d + \gamma) + \gamma pb}{d} < K$  i.e., all the coefficients  $A_0, A_1, A_2$  and  $A_3$  have negative sign. Therefore, according to Lemma A.1, Eq. (24) has no positive solution. As a consequence, Equations (21) and (23) ensure that the system (4) has no endemic equilibrium under the condition (A) of Theorem 3.2.

(B) We examine the possible number of positive roots using applying Lemma A.1 in Eq. (24). In Table 2, we have shown the sign of the coefficients of Eq. (24) under the different parametric conditions. Therefore, the number of positive roots and number of endemic fixed points of system (24) can be determined with the help of Equations (21) and (23).

Parametric conditions	$A_0$	$A_1$	$A_2$	$A_3$	Number of positive roots of Eq. (24)
B case-1(i)	+	-	+	-	three
B case-1(ii)	-	-	+	-	two
B case-2(a) 1(i)	-	+	-	-	two
B case-2(a) 1(ii)	-	-	+	-	two
B case-2(a) 1(iii)	-	+	+	-	two
B case-2(a) 2	-	-	-	-	nil
B case-2(b) 1(i)	+	+	-	-	unique
B case-2(b) 1(ii)	+	+	+	-	unique
B case-2(b) 1(iii)	+	-	-	-	unique
B case-2(b) 2	+	-	+	-	three

Table 2: Table indicates the sign of coefficients of Eq. (24) under the parametric conditions mentioned in Theorem 3.2 (B).

□

It is very difficult to express the positive root of Eq. (24) analytically. Therefore, we are not able to provide the analytical expression for the interior equilibrium point of system (20). However, we investigate the possible number of interior equilibrium points numerically. It is identified that the model system (4) possess at most two interior equilibrium points for particular set of parameters values from [37]. Let us consider the following set of parametric values for numerical investigation:

$$p = 0.2, b = 0.9, d = 0.3, \alpha = 0.4, \gamma = 0.4, \mu = 0.01, K = 0.04, r = 0.2, k = 0.65. \quad (26)$$

The following points explore the number of interior equilibrium point(s) for the set of parametric values (26):

- (i) For  $k = 0.4$ , Eq. (24) has no positive root which results that the model system (4) has no interior equilibrium point.
- (ii) For  $k = 0.5761804185$ , Eq. (24) has two positive roots namely,  $I_1 = 0.6223$ , and  $I_2 = 8.8150$  but  $I_2$  does not satisfy the positiveness condition of (23). Hence, the model system (4) generates unique interior equilibrium  $E_{sn}^* = (2.0545, 0.6223, 0.3232)$ .
- (iii) We increase the value of  $k$ , and at  $k = 0.7$ , Eq. (24) has three positive roots  $I_1 = 1.1551$ ,  $I_2 = 0.2474$  and  $I_3 = 6.4761$ . However, the positivity of (23) is not satisfied for  $I_3$ . Therefore, model system (4) exhibits two interior equilibrium points, namely,  $E_1^* = (1.5142, 0.1.1551, 0.3308)$  and  $E_2^* = (2.4347, 0.2474, 0.3178)$ .

The existence of interior equilibria of model system (4) with both the treatment functions is summarized in the Table 3:

Treatment functions	no interior equilibrium	one interior equilibrium	two interior equilibria
$T(I)=rI$	$\mathcal{R}_0 < 1$	$\left(\frac{\mu+r+d+\gamma}{d+\gamma}\right)^2 < \frac{\alpha}{\mathcal{R}_0-1}$ and $\mathcal{R}_0 > 1$	$\left(\frac{\mu+r+d+\gamma}{d+\gamma}\right)^2 > \frac{\alpha}{\mathcal{R}_0-1}$ $\mathcal{R}_0 > 1$
$T(I)=K$	Theorem 3.2	Theorem 3.2	Theorem 3.2

Table 3: Existence of interior equilibria for the model system (4).

For  $T(I) = K$ , the parameter  $k$  (disease contact rate) has significant impact on the change of number of endemic equilibrium point(s) of model system (4). Numerically, we prove that the model system (4) undergoes a saddle node bifurcation with respect to parameter  $k$  i.e., the number of endemic equilibrium point vary from zero to two with change in parameter  $k$ . Threshold value and transversality conditions of saddle-node bifurcation will be derived in Section 5.

## 4 Stability of equilibria

In this section, local and global stability of equilibrium points of model system (4) are studied. First we show the local stability of  $E^0$ .

**Theorem 4.1.** *Disease-free equilibrium  $E^0$  is unstable if  $\mathcal{R}_0 > 1$  while it is locally asymptotically stable if  $\mathcal{R}_0 < 1$ .*

*Proof.* We provide the proof in Appendix A.1. □

**Theorem 4.2.** *Local asymptotic stability of interior equilibrium point(s) of model system (4) is described as follows:*

1. *For the case  $T(I) = rI$ , interior equilibrium  $E^*(S^*, I^*, R^*)$  (whenever exists), is locally asymptotically stable if  $\sigma_1 > 0$ ,  $\sigma_2 > 0$ ,  $\sigma_3 > 0$ ,  $\sigma_1\sigma_2 - \sigma_3 > 0$ .*
2. *For the case  $T(I) = K$  interior equilibrium  $E^*(S^*, I^*, R^*)$  (whenever exists), is locally asymptotically stable if  $\sigma_1 > 0$ ,  $\sigma_2 > 0$ ,  $\sigma_3 > 0$ ,  $\sigma_1\sigma_2 - \sigma_3 > 0$ .*

*Proof.* We have reported the proof and expression  $\sigma_1$ ,  $\sigma_2$  and  $\sigma_3$  Appendix A.2. □

**Theorem 4.3.** *If  $\mathcal{R}_0 < \frac{d+\mu}{d+\mu+r}$  and  $K > \frac{b(1-p)(d+\gamma)+\gamma pb-Kd}{d}$ , then the disease-free equilibrium  $E^0$  of model system (4) is globally asymptotically stable.*

*Proof.* The proof of Theorem 4.3 is given in Appendix A.3.  $\square$

**Theorem 4.4.** For  $T(I) = rI$ , the model system (4) has a unique endemic equilibrium point  $E^*(S^*, I^*, R^*)$  when  $\mathcal{R}_0 > 1$  and it is globally asymptotically stable when  $\min\{(2d + \mu + r - \gamma - k\alpha), (d + \gamma - \mu - r - k\alpha)\} > 0$ .

*Proof.* We have reported the proof of the Theorem 4.4 in Appendix A.4.  $\square$

Based on the analysis of existence and stability of disease-free and interior equilibrium points for both the treatment functions  $T(I) = rI$  and  $T(I) = K$ , we conclude the following important results:

**Remark 1.** Basic reproduction number  $\mathcal{R}_0$  and the maximal capacity of treatment  $K$  are two critical terms which determine whether model system (4) has an endemicity or not. Theorem 4.3 ensures that for the treatment function  $T(I) = rI$ , disease-free equilibrium ( $E^0$ ) is globally asymptotically stable when  $\mathcal{R}_0 < 1$ . For  $\mathcal{R}_0 > 1$ , Theorem 3.1(i) and Theorem 4.2(1) ensure that a unique endemic equilibrium  $E^*(S^*, I^*, R^*)$  emerges for the treatment function  $T(I) = rI$ , which is locally asymptotically stable when  $\sigma_1 > 0$ ,  $\sigma_2 > 0$ ,  $\sigma_3 > 0$ ,  $\sigma_1\sigma_2 - \sigma_3 > 0$ .

**Remark 2.** Theorem 3.2(A) make sure that if  $\mathcal{R}_0 < \frac{d+\mu}{d+\mu+r}$  and  $K > \frac{b(1-p)(d+\gamma)+\gamma pb-Kd}{d}$ , model system (4) has no endemic equilibrium and for  $\mathcal{R}_0 < \frac{d+\mu}{d+\mu+r} (< 1)$ , model system (4) exhibits backward bifurcations for the treatment function  $T(I) = K$ . **Thus the large maximal capacity of treatment  $K$  could help the elimination of disease outbreak for the treatment function  $T(I) = K$ .**

**Remark 3.** Theorem 4.4 provides sufficient conditions when model system (4) with  $T(I) = rI$  may exhibit a unique endemic equilibrium  $E^*(S^*, I^*, R^*)$  that is globally asymptotically stable. The model system (4) with  $T(I) = K$  undergoes a saddle-node bifurcation with respect to the disease contact rate  $k$ .

Treatment functions	$T(I) = rI$		$T(I) = K$
Parametric values	$r = 0.25$	$r = 0.65$	$K = 0.04$
$\mathcal{R}_0$	0.4902 (< 1)	1.2745 (> 1)	1.2745 (> 1)
Disease-free equilibrium	$E^0(2.7429, 0, 0.2571)$	$E^0(2.7429, 0, 0.2571)$	$E^0(2.7429, 0, 0.2571)$
Eigenvalues	-0.31, -0.3, -0.26	-0.31, -0.3, 0.14	
Nature	stable	unstable	unstable
Interior equilibria	does not exist	$E^*(1.3206, 1.0940, 0.5854)$	$E_1^*(1.0505, 1.6123, 0.3372)$ , $E_2^*(2.5128, 0.3752, 0.3186)$
Eigenvalues		-0.1339, -0.4388 + 0.2571 <i>i</i> , -0.4388 - 0.2571 <i>i</i>	at $E_1^*$ , - 0.0077, -0.30, -0.6986, at $E_2^*$ , 0.3251, -0.30, -0.70
Nature		stable	$E_1^*$ is stable, $E_2^*$ is saddle

Table 4: Table summarize the existence and stability of equilibria of model system (4) for different intensity of  $r$  (when  $T(I) = rI$  is included) and  $K$  (when  $T(I) = K$  is included) and other parameters values are reported in (26).

## 5 Bifurcation analysis

In this section, we present the bifurcation analysis of model system (4) with both the treatment functions  $T(I) = rI$  and  $T(I) = K$ . We mainly describe that how the interior equilibrium point(s) appears or disappears with bifurcation parameters.

### 5.1 Transcritical bifurcation

In the Section 3 and Section 4, we observe that the unique endemic equilibrium appear for  $\mathcal{R}_0 > 1$  and the model system (4) does not possess endemic equilibrium for  $\mathcal{R}_0 < 1$  when treatment function  $T(I) = rI$ . We have identified that the disease-free equilibrium ( $E^0$ ) is stable for  $\mathcal{R}_0 < 1$  and become saddle point for  $\mathcal{R}_0 > 1$ . Here, model system (4) with  $T(I) = rI$  produces transcritical bifurcation for parameter  $k$  which influences  $\mathcal{R}_0$ .

**Proposition 5.1.** *The model system (4) undergoes a transcritical bifurcation at  $k_T = d + \mu + r$  and  $E^0$  changes its stability from stable to unstable (cf. Figure 3).*

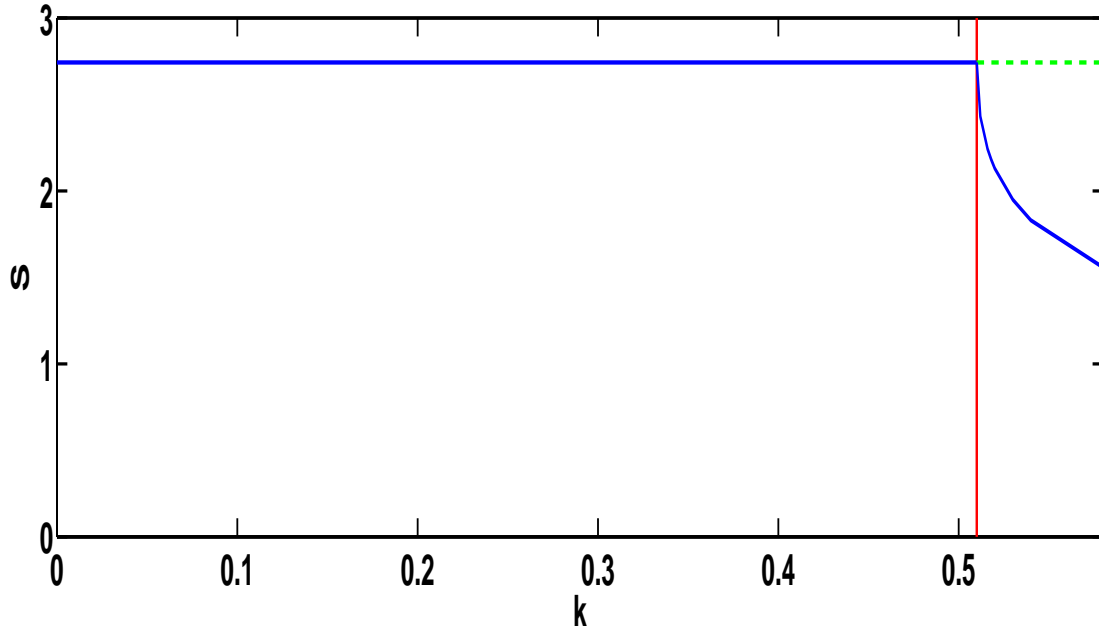


Figure 3: It illustrates the transcritical bifurcation with respect to  $k$  and parameters value are reported in (26). Bifurcation parameter  $k$  is plotted on horizontal axis and  $S$ -component of equilibrium (disease-free and interior) is plotted on vertical axis. Stable and saddle disease-free equilibrium are depicted by blue and dotted green colored horizontal lines. Blue colored curve depicts stable interior equilibrium. Red colored vertical line is the threshold at  $k_T = 0.51$ .

We numerically show that the model system (4) undergoes a transcritical bifurcation at  $k_T$ . We choose the parameter values same as (26) and see that the model system exhibits a transcritical bifurcation at the threshold  $k_T = 0.51$ , where disease-free equilibrium switches stability along with appearance or disappearance of interior equilibria in the presence of treatment strategy  $T(I) = rI$  (cf. Figure 3). In Figure 3, left side of  $k_T$ , no interior equilibria appear and disease-free equilibrium point is globally stable. In the right side of  $k_T$ , disease-free equilibrium loses its stability and become saddle, and unique endemic equilibrium point appears.

## 5.2 Saddle-node bifurcation

This subsection investigate saddle-node bifurcation with respect to the parameter  $k$  for model system (4) with treatment function  $T(I) = K$ . In Section 3, we have examined that the parameter  $k$  is responsible for the appearance/disappearance of interior equilibria. Here we derive the transversality conditions [56] for saddle-node bifurcation induced by the parameter  $k$ . Let  $k_{sn}$  be the threshold parameter value of  $k$  for saddle-node bifurcation. Therefore, model system (4) has no endemic equilibrium below  $k_{sn}$  and two endemic equilibria beyond  $k_{sn}$ . At  $k_{sn}$ , two equilibrium points collide to a unique equilibrium and it is denoted by  $E_{sn}(S_{sn}, I_{sn}, R_{sn})$  (cf

Figure 4). Define  $F(S, I, R) = [F_1(S, I, R), F_2(S, I, R), F_3(S, I, R)]^T$ , where

$$\begin{aligned} F_1(S, I, R) &= (1-p)b - dS - \frac{kIS^2}{S^2 + \alpha I^2} + \gamma R, \\ F_2(S, I, R) &= \frac{kIS^2}{S^2 + \alpha I^2} - (d + \mu)I - T(I), \\ F_3(S, I, R) &= pb + \mu I - (d + \gamma)R + T(I). \end{aligned} \quad (27)$$

Now differentiating  $F$  with respect to  $k$ , we obtain

$$F_k(E_{sn}; k_{sn}) = \begin{pmatrix} F_{1k}(E_{sn}; k_{sn}) \\ F_{2k}(E_{sn}; k_{sn}) \\ F_{3k}(E_{sn}; k_{sn}) \end{pmatrix} = \begin{pmatrix} -\frac{I_{sn}S_{sn}^2}{S_{sn}^2 + \alpha I_{sn}^2} \\ \frac{I_{sn}S_{sn}^2}{S_{sn}^2 + \alpha I_{sn}^2} \\ 0 \end{pmatrix}.$$

The transversality conditions for the aforesaid bifurcation are given by

$$W^T F_k(E_{sn}; k_{sn}) = \frac{I_{sn}S_{sn}^2}{S_{sn}^2 + \alpha I_{sn}^2} (w_2 - w_1),$$

$$\begin{aligned} W^T [D^2 F((E_{sn}; k_{sn}))(V, V)] &= \left( \frac{2k_{sn}I_{sn}}{S_{sn}^2 + \alpha I_{sn}^2} - \frac{10k_{sn}I_{sn}S_{sn}^2}{(S_{sn}^2 + \alpha I_{sn}^2)^2} + \frac{8k_{sn}I_{sn}S_{sn}^4}{(S_{sn}^2 + \alpha I_{sn}^2)^3} \right) (w_2 - w_1)v_1^2 \\ &+ \left( \frac{6k_{sn}S_{sn}^2\alpha I_{sn}}{(S_{sn}^2 + \alpha I_{sn}^2)^2} - \frac{8k_{sn}I_{sn}^3S_{sn}^2\alpha^2}{(S_{sn}^2 + \alpha I_{sn}^2)^3} \right) (w_1 - w_2)v_2^2 \\ &+ \left( \frac{2k_{sn}S_{sn}}{S_{sn}^2 + \alpha I_{sn}^2} - \frac{4k_{sn}\alpha I_{sn}^2 S_{sn} + 2k_{sn}S_{sn}^3}{(S_{sn}^2 + \alpha I_{sn}^2)^2} \right. \\ &\left. + \frac{8k_{sn}\alpha I_{sn}^2 S_{sn}^3}{(S_{sn}^2 + \alpha I_{sn}^2)^3} \right) (w_2 - w_1)v_1v_2, \end{aligned}$$

where  $V = (v_1, v_2, v_3)^T$  and  $W = (w_1, w_2, w_3)^T$  are the eigenvectors of Jacobian matrix  $J|_{(E_{sn}; k_{sn})}$  and  $J^T|_{(E_{sn}; k_{sn})}$ , respectively. Since it is difficult to find out the analytical expression of endemic equilibrium point(s), we numerically validate the saddle-node bifurcation for  $K = 0.04$  and other parameter values are reported in (26). For this set of parameter values, model system (4) has two endemic equilibrium points given by  $E_1^* = (1.0505, 1.6123, 0.3372)$  and  $E_2^* = (2.5128, 0.3752, 0.3186)$ . If we decrease the parameter  $k$ , then at threshold value  $k_{sn} = 0.5761804185$ , two endemic equilibria collide at  $E_{sn}^* = (2.0545, 0.6223, 0.3232)$ . Eigenvectors corresponding to eigenvalue  $\lambda = 0$  for Jacobian matrix  $J|_{(E_{sn}; k_{sn})}$  and  $J|_{(E_{sn}; k_{sn})}^T$  are given by  $V = [-1.68654, 1.67367, 0.01287]^T$  and  $W = [0.80686, 2.21888, 0.62066]^T$ , respectively. The first transversality condition for saddle-node bifurcation is  $W^T F_k(E_{sn}; k_{sn}) = 1.134 (\neq 0)$  and second transversality condition is  $W^T [D^2 F(E_{sn}; k_{sn})](V, V) = -3.258 (\neq 0)$ . Therefore, the model system (4) undergoes saddle-node bifurcation at  $k = k_{sn} = 0.87022010232406$ .

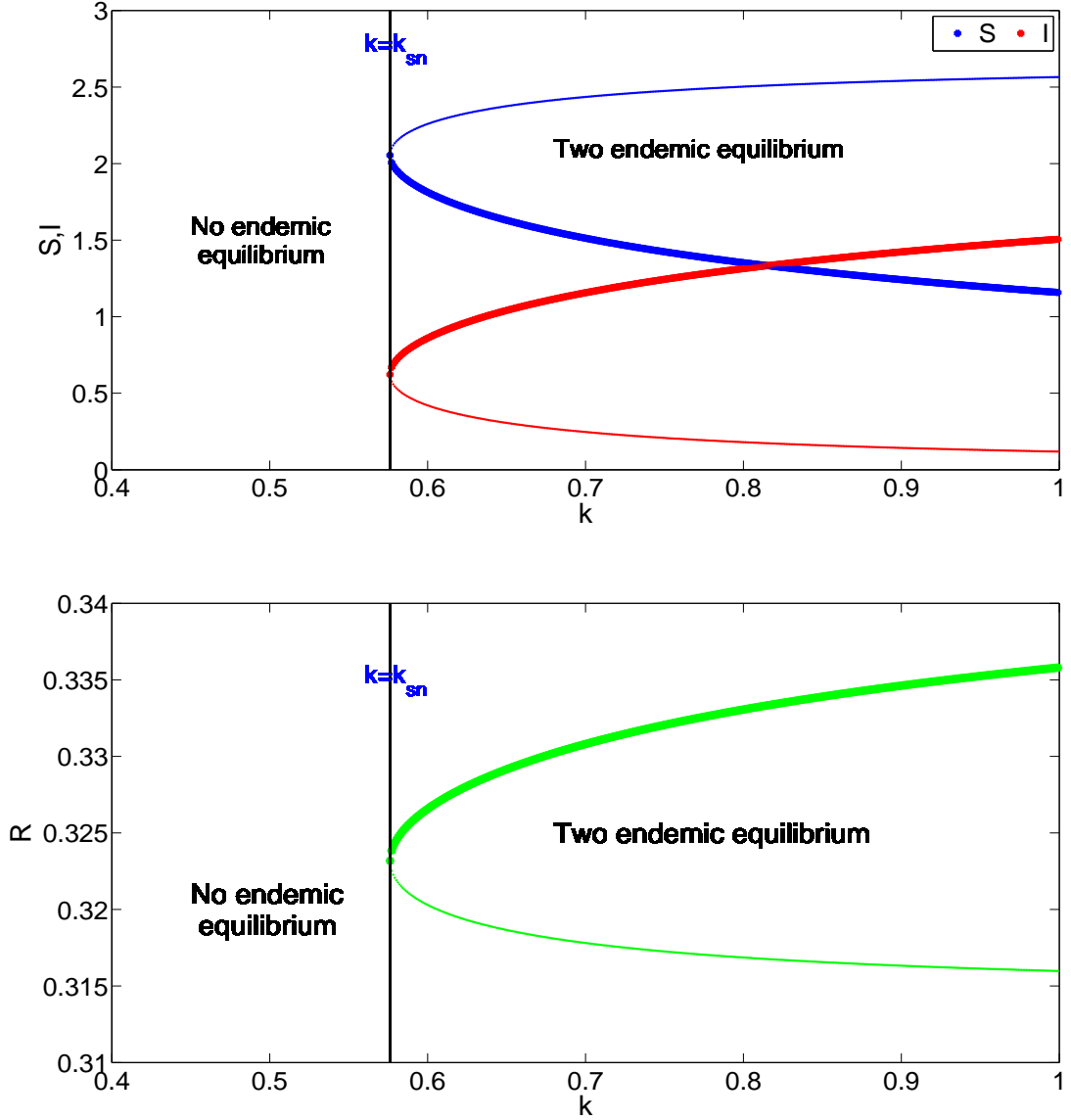


Figure 4: It depicts the saddle-node bifurcation of model system (4) with the treatment function  $T(I) = K$  for the bifurcation parameter  $k$  and other parametric values are taken from (26), where bold curve represents the endemic equilibrium  $E_1^*$  and thin curve represents the endemic equilibrium  $E_2^*$ .

Further, we investigate the local stability of the both endemic equilibrium (whenever exist) of model system (4) with treatment function  $T(I) = K$ . We plot the maximum of real parts of eigenvalues ( $\max(\Re(\lambda))$ ) of the both Jacobian matrices corresponding  $E_1^*$  and  $E_2^*$  with respect to the parameter  $k$  and other parametric values are fixed same as (26). In Figure 5, we observe that  $\max(\Re(\lambda))$  of the Jacobian at  $E_2^*$  is always positive, therefore, endemic equilibrium  $E_2^*$  is unstable (whenever exists) (see red colored curve). Further,  $\max(\Re(\lambda))$  of the Jacobian at  $E_1^*$  is positive when  $k_{sn} < k \leq k_* = 0.6459$  and is negative when  $k > k_*$ . Therefore, for set of parametric values

same as (26), the endemic equilibrium  $E_1^*$  is stable when  $k_{sn} < k \leq k_* = 0.6459$  and unstable when  $k > k_*$ . Further, we observe that model system (4) has a unique endemic equilibrium  $E_{sn}^*$  at  $k = k_{sn}$ , which is always unstable.

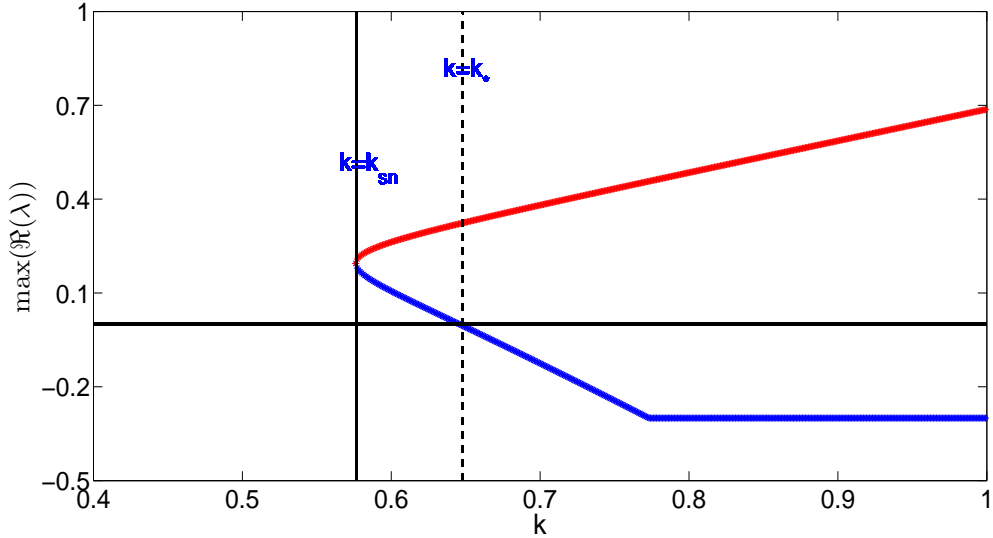


Figure 5: It illustrates the local stability of both endemic equilibrium points of model system (4) with treatment function  $T(I) = K$ . The red colored curve represents the  $\max(\Re(\lambda))$  of the Jacobian at endemic equilibrium  $E_2^*$  and blue colored curve represents the  $\max(\Re(\lambda))$  of the Jacobian at endemic equilibrium  $E_1^*$ .

## 6 Sensitivity analysis

### 6.1 Local sensitivity analysis of $R_0$

The sensitivity analysis determines the relative importance of the different parameters in connection to  $R_0$ . The perturbation of fixed point estimation of model parameters and the uncertainty in the model parameter estimation are the two most commonly used techniques for sensitivity analysis. The sensitivity of a variable with respect to model parameters is usually measured by sensitivity index. Sensitivity indices enable us to quantify the relative change in a variable when a parameter changes. For example if we consider  $k$ , which is one of the parameters in  $R_0$  and let  $\delta > 0$  be a small perturbation corresponding to  $k$ , then we have

$$\delta_{R_0} = R_0(k + \delta) - R_0(k) = \delta \frac{R_0(k + \delta) - R_0(k)}{\delta} \approx \delta \frac{\partial R_0}{\partial k}.$$

We define the normalized sensitivity indices ( $si$ ) as

$$si_k = \frac{k}{R_0} \frac{\partial R_0}{\partial k}.$$

For example,  $si_k = 1$  indicates that an increase (decrease) of  $k$  by  $y\%$  increases (decreases)  $R_0$  by  $y\%$ . On the other hand,  $si_k = -1$  indicates that an increase (decrease) of  $k$  by  $y\%$  decreases (increases)  $R_0$  by  $y\%$ . In this case,  $k$  is called a most sensitive parameter. Further, we compute

$$si_k = 1, \quad si_d = \frac{-d}{(d + \mu + r)^2}, \quad si_\mu = \frac{-\mu}{(d + \mu + r)^2}, \quad si_r = \frac{-r}{(d + \mu + r)^2}.$$

Consider the parametric values same as (26) and compute the sensitivity indices in the Table 5.

Parameter	Sensitivity indices of $R_0$
$k$	1
$d$	-0.59512
$\mu$	-0.03844
$r$	-0.76893

Table 5: Sensitivity analysis of  $R_0$

The sensitivity indices related to  $k$  is positive and remaining three are negative as defined in Table 5. From Table 5,  $si_r = -0.76893$ ; which tells that increasing (decreasing)  $r$  by 10% decreases (increases)  $R_0$  by 7.6893%. A highly sensitive parameter should carefully be estimated, because a small variation in that parameter will lead to large quantitative changes. As it can be easily observed from Table 5, the basic reproduction number is most sensitive to the transmission rate  $k$ . **Therefore an increase in the transmission rate  $k$  increases the spread of disease in the community.**

## 6.2 Global sensitivity analysis

In this section, we perform global sensitivity analysis using the methodology of Latin Hypercube Sampling (LHS) and partial sensitivity analysis (PRCCs) to examine the dependence of  $R_0$  on parameters. We also perform the sensitivity of parameters on the infected population for both the treatment functions  $T(I) = rI$  and  $T(I) = K$ . LHS is a stratified sampling without replacement technique which allows for an efficient analysis of parameter variations across simultaneous uncertainty ranges in each parameter [57]. PRCC measures the strength of the relationship between the model outcome and the parameters, stating the degree of the effect that each parameter has on the outcome. Thus, sensitivity analysis determines the parameters with the most significant impact on the outcome of the numerical simulation of the model system. Note that the PRCC values remains between -1 and 1. Positive (negative) values indicate a positive (negative) correlation of the parameter with the model output. A positive (negative) correlation implies that a positive (negative) change in the parameter will increase (decrease) the model output. The larger the absolute value of the PRCC, the greater the correlation of the parameter

with the output. To generate the LHS matrices, we assume that all the parameters are uniformly distributed. Then using the baseline values same as (26), a total 1000 simulations of the system (4) were carried out. From Figure 6(a), we observe that the disease contact rate  $k$  and treatment rate  $r$  are most sensitive parameter and from Figure 6(b), we observe that the disease contact rate  $k$  and maximal capacity of treatment  $K$  are most sensitive parameter. Figure 6(c) demonstrates that the disease contact rate  $k$  and treatment rate  $r$  are most sensitive parameter on  $R_0$ .

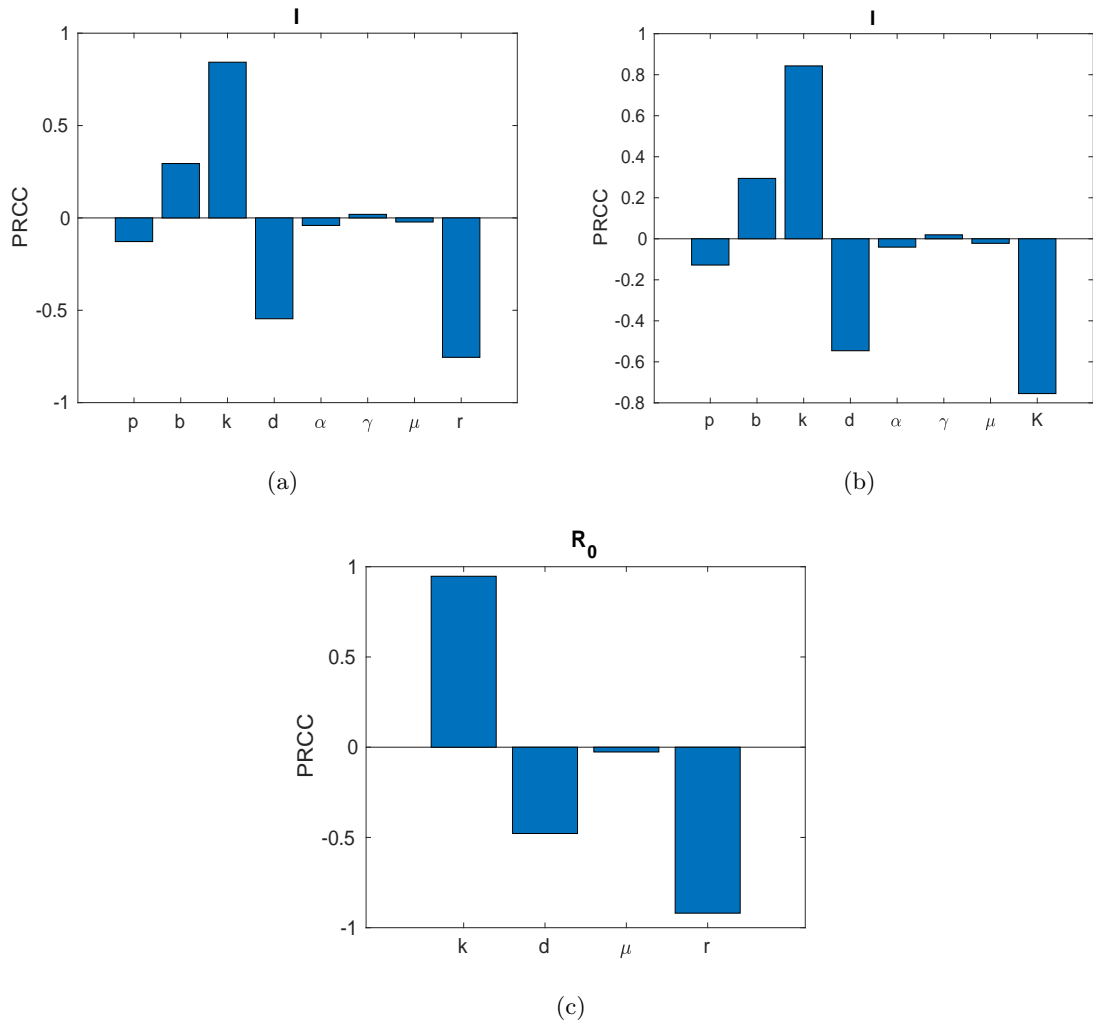


Figure 6: (a) PRCC sensitivity on I, for  $T(I) = rI$ . (b) PRCC sensitivity on I, for  $T(I) = K$ . (c) PRCC sensitivity on  $R_0$ .

### 6.3 Sensitivity analysis of the point of endemic equilibrium

In this subsection, we performed the sensitivity analysis of stable endemic fixed point. We identify which parameters are important in contributing variability in the outcome of the endemic fixed point.

### 6.3.1 Sensitivity indices of model parameters for $T(I)=rI$

We demonstrate the sensitivity indices of the model parameters when proportional treatment  $T(I)=rI$  is incorporated in the model system (5). In order to determine the sensitivity indices of the model parameters, we adopt the procedure described in Chitnis et al. [65,66]. To do this, we replace the variables (S,I,R) to  $(s_1, s_2, s_3)$ , parameters (p, b, d, k,  $\alpha$ ,  $\gamma$ ,  $\mu$ , r) to  $(y_1, y_2, y_3, y_4, y_5, y_6, y_7, y_8)$  and coexistence fixed point  $(S^*, I^*, R^*)$  by  $(s_1^*, s_2^*, s_3^*)$ . We have the following equilibrium equation:

$$\begin{aligned} f_i(s_1, s_2, s_3; y_1, y_2, y_3, y_4, y_5, y_6, y_7, y_8) &= 0, i = 1, 2, 3. \\ f_1(s_1, s_2, s_3; y_1, y_2, y_3, y_4, y_5, y_6, y_7, y_8) &= (1 - y_1)y_2 - y_3s_1 - \frac{y_4s_2s_1^2}{s_1^2 + y_5s_2^2} + y_6s_3 = 0, \\ f_2(s_1, s_2, s_3; y_1, y_2, y_3, y_4, y_5, y_6, y_7, y_8) &= \frac{y_4s_2s_1^2}{s_1^2 + y_5s_2^2} - (y_3 + y_7)s_2 - y_8s_2 = 0, \\ f_3(s_1, s_2, s_3; y_1, y_2, y_3, y_4, y_5, y_6, y_7, y_8) &= y_1y_2 + y_7s_2 - (y_3 + y_6)s_3 + y_8s_2 = 0. \end{aligned} \quad (28)$$

Let

$$AX_j = -K_j, \quad (29)$$

where

$$\begin{aligned} A &= \begin{bmatrix} a_{11} & a_{12} & a_{13} \\ a_{21} & a_{22} & a_{23} \\ a_{31} & a_{32} & a_{33} \end{bmatrix}, \quad X_j = \begin{bmatrix} \frac{\partial s_1^*}{\partial y_j} \\ \frac{\partial s_2^*}{\partial y_j} \\ \frac{\partial s_3^*}{\partial y_j} \end{bmatrix}, \quad K_j = \begin{bmatrix} -\frac{\partial f_1}{\partial y_j} \\ -\frac{\partial f_2}{\partial y_j} \\ -\frac{\partial f_3}{\partial y_j} \end{bmatrix}; \\ a_{11} &= -y_3 - \frac{2y_4s_2^*s_1^*}{(s_2^{*2}y_5 + s_1^{*2})} + \frac{2y_4s_2^{*3}s_1^{*3}}{(s_2^{*2}y_5 + s_1^{*2})^2}, \quad a_{12} = -\frac{y_4s_1^{*2}}{(s_2^{*2}y_5 + s_1^{*2})} + \frac{2y_4s_2^{*2}s_1^{*2}y_5}{(s_2^{*2}y_5 + s_1^{*2})^2}, \\ a_{13} &= y_6, \quad a_{21} = \frac{2y_4s_2^*s_1^*}{(s_2^{*2}y_5 + s_1^{*2})} - \frac{2y_4s_2^{*3}s_1^{*3}}{(s_2^{*2}y_5 + s_1^{*2})^2}, \\ a_{22} &= \frac{y_4s_1^{*2}}{(s_2^{*2}y_5 + s_1^{*2})} - \frac{2y_4s_2^{*2}s_1^{*2}y_5}{(s_2^{*2}y_5 + s_1^{*2})^2} - y_3 - y_7 - y_8, \quad a_{23} = 0 \\ a_{31} &= 0, \quad a_{32} = y_7 + y_8, \quad a_{33} = -y_3 - y_6. \end{aligned} \quad (30)$$

Finally, the sensitivity index of the point of coexistence equilibrium,  $s_i^*$ , to the parameter,  $y_j$  is given by

$$\frac{\partial s_i^*}{\partial y_j} \cdot \frac{y_j}{s_i^*}, \quad 1 \leq i \leq 3 \quad \text{and} \quad 1 \leq j \leq 8. \quad (31)$$

Sensitivity indices of the model parameters for fixed coexistence point are obtained in the following Table 6. We have provided the details calculation of sensitivity indices in Appendix A.5. Table 6 assure that most sensitive parameter for  $S^*$  is k followed by b,r,d, $\alpha$ , $\gamma$ ,p, $\mu$ ; parameter d is the most sensitive parameter for  $I^*$  followed by k,b,r, $\alpha$ , $\gamma$ ,p, $\mu$ ; and d is the most sensitive parameter for  $R^*$  followed by b,k, $\gamma$ ,p,r, $\alpha$ , $\mu$ .

Parameter	$S^*$	$I^*$	$R^*$
p	-0.09374999995	-0.09374999998	0.386731146
b	0.9999999990	0.9999999995	1
d	-0.2942219741	-1.659768193	-1.359208355
k	-1.203713850	1.117714722	0.6267059447
$\alpha$	0.2592614446	-0.2407385555	-0.1349828189
$\gamma$	0.1219480732	0.1219480732	-0.5030519267
$\mu$	0.01790417863	-0.02761402866	0.01121687319
r	0.3580835726	-0.5522805733	0.2243374638

Table 6: Sensitivity indices of the parameters of model (5) for the stable endemic equilibrium.

### 6.3.2 Sensitivity indices of model parameters for constant treatment $T(I)=K$

We adopt the same procedure to determine the sensitivity indices of the model parameters as discussed in subsection 6.3.1 when constant treatment is incorporated in the system. For the parameters value mentioned in (26), we provide the sensitivity indices of the model parameters in the Table 7. Table 7 indicates that most sensitive parameter for  $S^*$  is b followed by k,d, $\alpha$ ,p, $\gamma$ ,K, $\mu$ ;

Parameter	$S^*$	$I^*$	$R^*$
p	-0.09115300447	-0.09869562105	0.7555884435
b	0.9722987147	1.052753292	0.8341955399
d	-0.4324219700	-1.468574393	-0.5288280417
k	-0.64706818917	0.4158523772	0.02838940343
$\alpha$	0.3137635375	-0.2016469285	-0.01376602928
$\gamma$	0.06832695962	0.07398079478	-0.5663780515
$\mu$	0.01116319934	-0.02125877872	0.06681669006
K	0.02770128601	-0.05275329155	0.1658044602

Table 7: Sensitivity indices of the parameters of model (5) for the stable endemic equilibrium.

parameter d is the most sensitive parameter for  $I^*$  followed by b,k, $\alpha$ ,p, $\gamma$ ,K, $\mu$ ; and b is the most sensitive parameter for  $R^*$  followed by p, $\gamma$ ,d,K, $\mu$ ,k, $\alpha$ .

## 7 Numerical Simulation

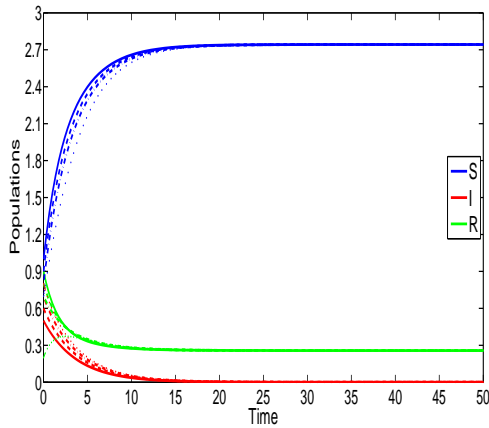
In this section, we perform numerical simulations to validate our theoretical finding. Treatment strategies, vaccination rate and infectious force function are the important factors to analyze the disease dynamics of model system (4). Treatments are provided either proportionally or constantly depending on the availability of infected population sizes. Infection force is affected by the disease contact rate k and psychological or inhibitory effect parameter  $\alpha$ . Therefore, we examine numerically how (i) different treatment functions; (ii) varied vaccination rates and (iii) the disease contact rate parameter in infection force function affect the endemicity. To address

these questions, we consider the same set of parametric values given in (26).

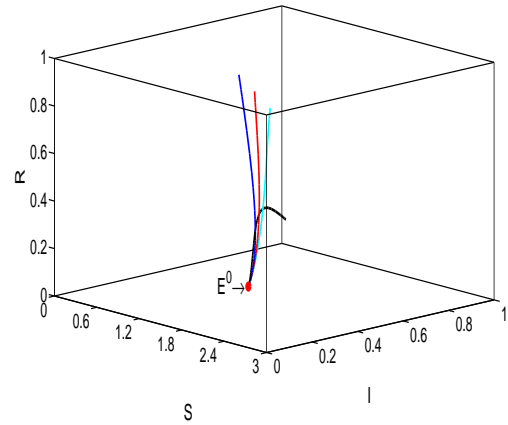
### 7.1 Effect of the treatment function and the vaccination rate:

We provide the treatment depending on availability of the infected individuals as described in Eq. (3). We choose parametric values from the Eq. (26) to investigate the effect of treatment strategies on the dynamic of model system (4). When the treatment function  $T(I) = rI$  is incorporated in model system (4), we choose  $k = 0.25$  and other parameter values are fixed from (26). Under this set of parametric values, for model system (4), the basic reproduction number  $\mathcal{R}_0 = 0.4902 < 1$ . Therefore according to Theorem 3.1, model system (4) has no interior equilibrium point and from Theorem 4.1, there exists a disease-free equilibrium  $E^0(2.7429, 0, 0.2571)$ , which is stable. The set of parametric values in (26) also satisfy the sufficient conditions mentioned in Theorem 4.3 for global asymptotic stability of disease-free equilibrium point (see, Figure 7). Therefore, Figure 7 provides a numerical example which shows that disease does not persist in the model system (4). Next we choose  $k = 0.65$  and other parametric values are taken from (26). For this set of parametric values, we obtain  $\mathcal{R}_0 = 1.2745 > 1$  which is consistent with Theorem 3.1(i). Therefore, the model system (4) generates one disease-free equilibrium point  $E^0(2.7429, 0, 0.2571)$  which is saddle and a unique interior equilibrium point  $E^*(1.3206, 1.0940, 0.5854)$  which is stable (cf. Figure 8).

When we take treatment function  $T(I) = K$  in model system (4), and choose the numerical values of parameters from (26). The model system (4) has two interior equilibrium points:  $E_1^*(1.0505, 1.6123, 0.3372)$  which is stable (refer the Fig. 9) and unstable interior equilibrium point  $E_2^*(2.5128, 0.3752, 0.3186)$ .

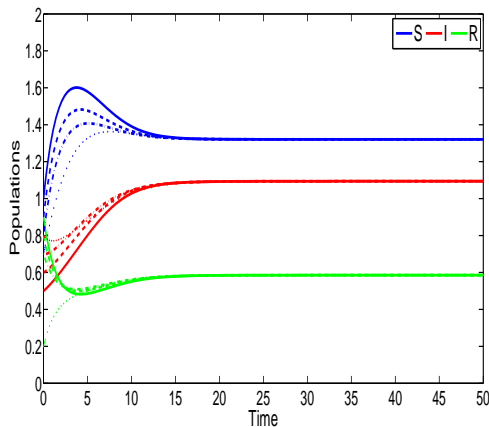


(a) Long term dynamics of solution of model system (4).

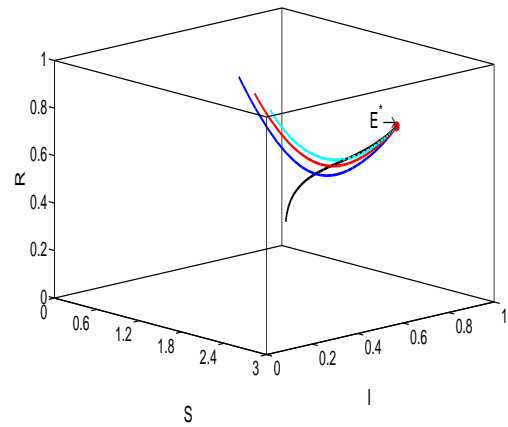


(b) Phase portrait of model system (4).

Figure 7: It illustrates the global stability of disease-free equilibrium point  $E^0(2.7429, 0, 0.2571)$  of model system (4) when treatment function  $T(I) = rI$ , where  $k = 0.25$  and other parametric values are reported in (26) and  $R_0 = 0.4902 < 1$ . Trajectories with different initial conditions are approaching to  $E^0$ .



(a) Long term dynamics of solution of model system (4).



(b) Phase portrait of model system (4).

Figure 8: It depicts the global stability of endemic equilibrium  $E^*(1.3206, 1.0940, 0.5854)$  of model system (4) when  $R_0 = 1.2745 > 1$ . The numerical value of parameters are given in (26). All the trajectories with different initial conditions are approaching to  $E^*$ .

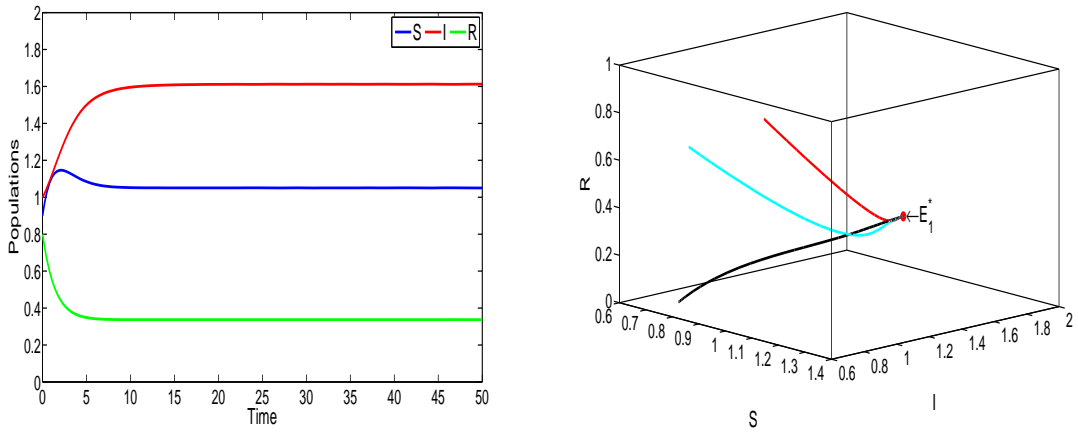


Figure 9: It shows the local stability of endemic equilibrium  $E_1^*(1.0505, 1.6123, 0.3372)$  of model system (4) with treatment function  $T(I) = K$ . The numerical values of parameters are given in (26).

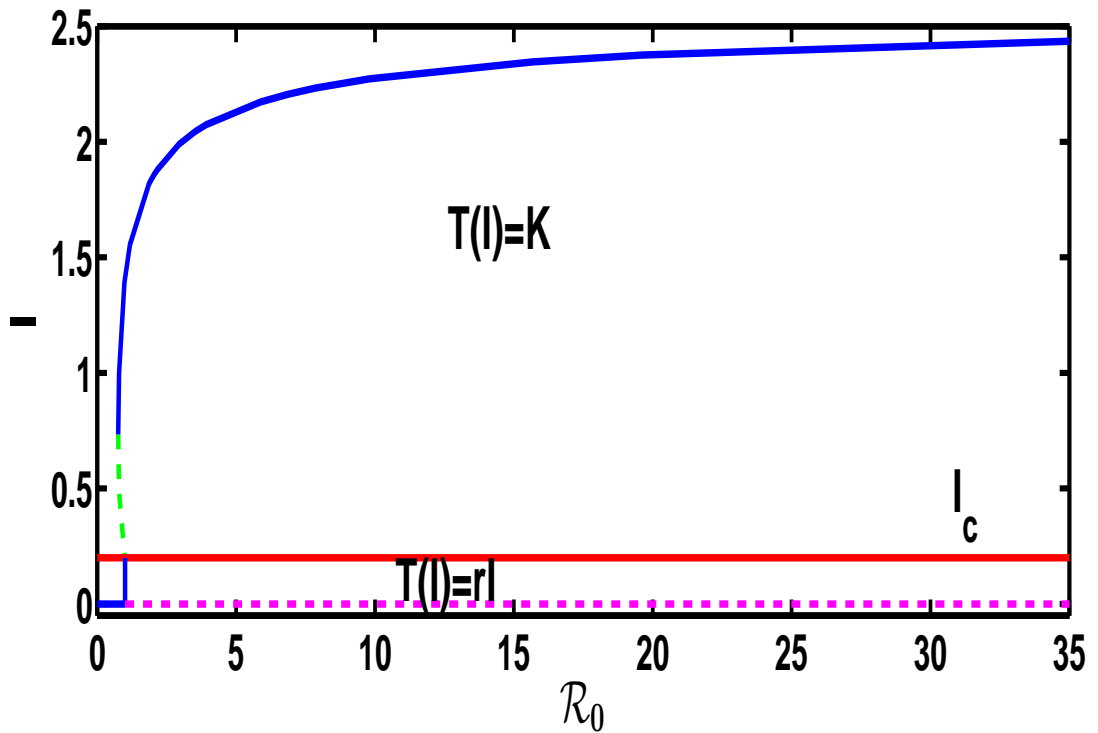
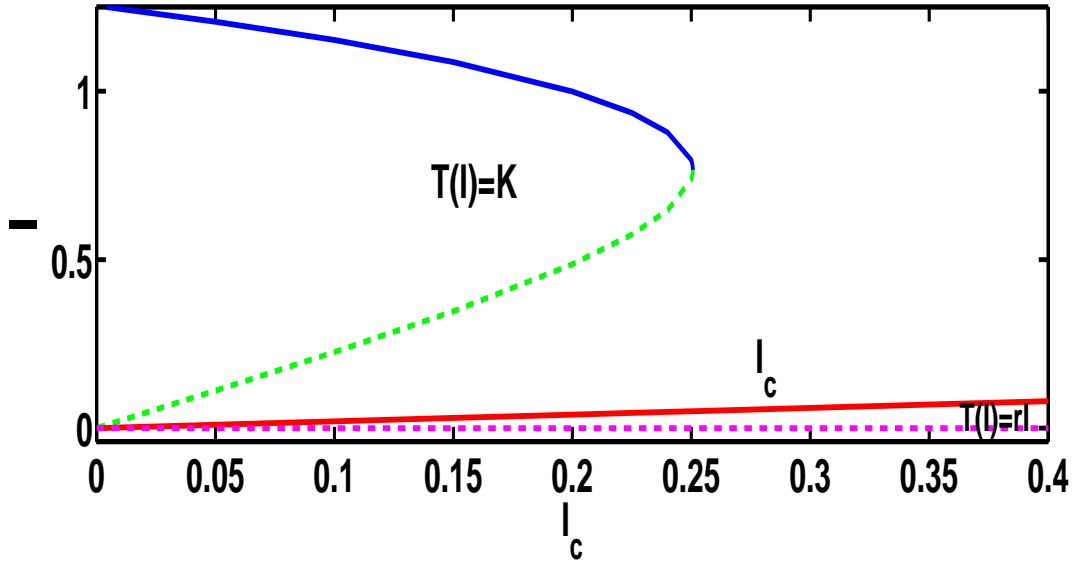


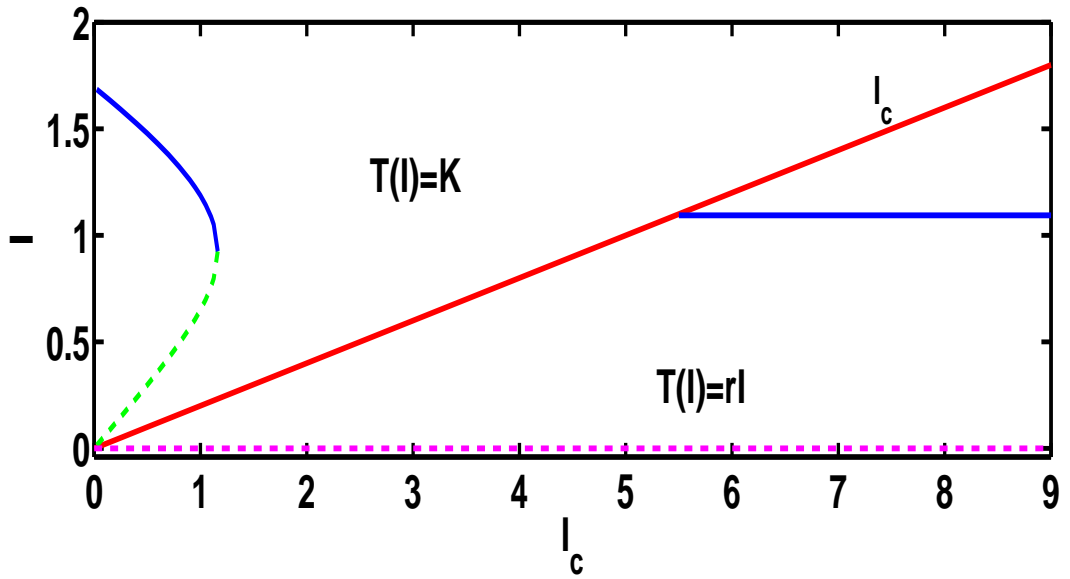
Figure 10: The bifurcation diagram of infected population size  $I$  vs. basic reproduction number  $\mathcal{R}_0$  of model system (4) when  $I_c = 4/20$  and other parametric values are given in (26). The blue colored curve denotes stable interior equilibrium; the green colored curve indicates saddle interior equilibrium; magenta colored horizontal line depicts disease free equilibrium and red colored line is  $I_c$ .

Figure 10 is the bifurcation diagram of the basic reproduction number  $\mathcal{R}_0$  versus infective size  $I$  of model system (4). Blue colored curve is stable interior equilibrium, green colored dotted

curve is saddle interior equilibrium point, magenta colored horizontal line is the disease free equilibrium and red colored horizontal line is  $I_c$ . In Figure 10, treatment strategy  $T(I) = K$  is included above the  $I_c$  line. In this case, model system produces two endemic interior equilibria. Highly infected equilibrium point is stable. Figure 10 suggests that infection level increases rapidly for low value of  $\mathcal{R}_0$  and further, it is increasing slowly. Treatment function  $T(I) = rI$  is included below the  $I_c$  line. Here, disease persists when  $\mathcal{R}_0 > 1$  as disease-free equilibrium point is unstable, and disease die out for  $\mathcal{R}_0 < 1$ .



(a)  $\mathcal{R}_0 = 0.7843137255 < 1$



(b)  $\mathcal{R}_0 = 1.27 > 1$

Figure 11: The bifurcation diagram of the infected population size of model system (4) vs. capacity of treatment. The blue colored curve shows the locally stable equilibrium; the green colored dotted curve indicates the saddle equilibrium; magenta colored dotted line depicts disease free equilibrium and red colored line is  $I_c$ .

Figure 11 illustrates bifurcation of the infected population size  $I$  vs. capacity of treatment  $I_c$  of model system (4). Description of Figure 11 is the same as discussed in Figure 10. Figure 11(a) and Figure 11(b) demonstrate the variation of infected population for  $\mathcal{R}_0 < 1$  and  $\mathcal{R}_0 > 1$ , respectively. In Figure 11(a), when  $\mathcal{R}_0 < 1$ , model system (4) has no infection for treatment

function  $T(I) = rI$ , but disease arises for treatment  $T(I) = K$ . For  $\mathcal{R}_0 > 1$ , disease persists in the both treatment functions. Figure 11 suggests that infected population decreases with respect capacity  $I_c$ . Adopting the high capacity results disease completely die out.

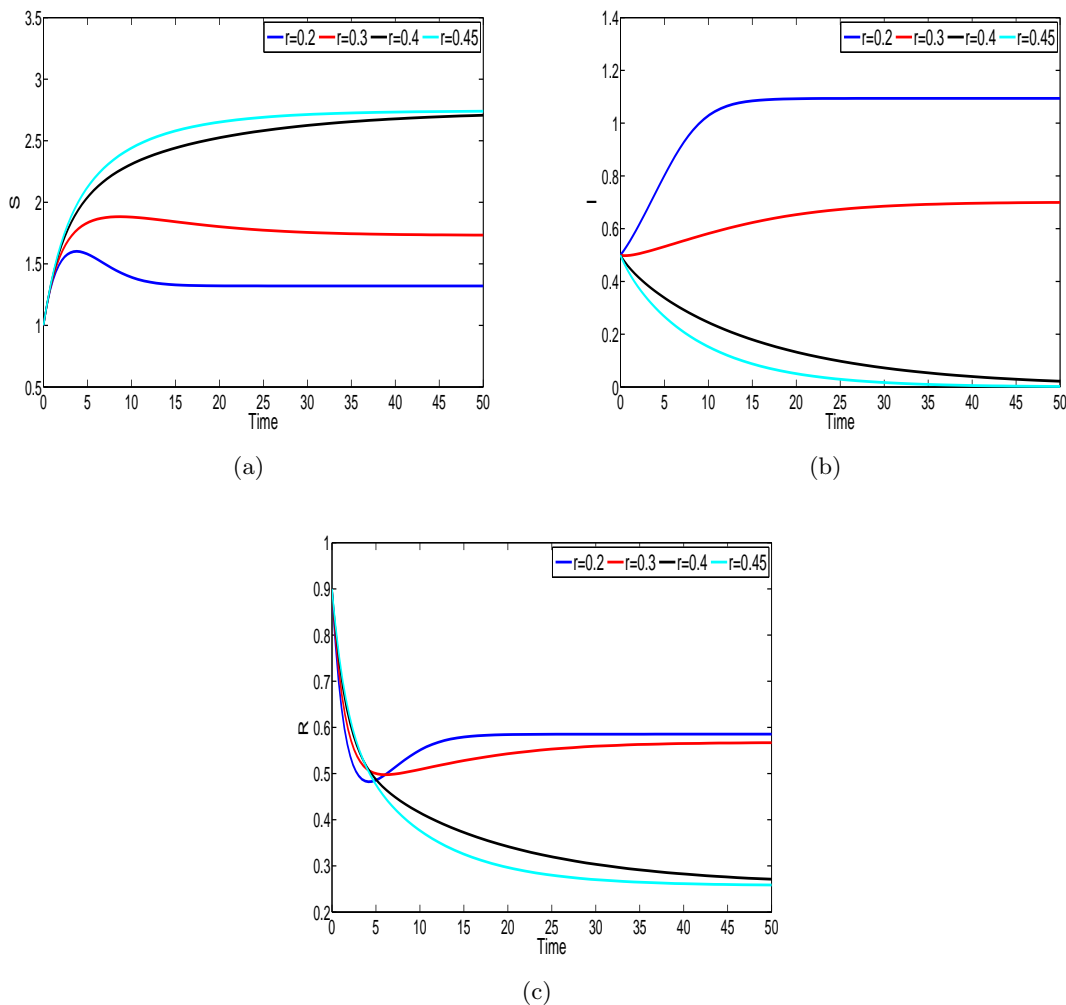


Figure 12: Dependence of  $S$ ,  $I$ , and  $R$  on the parameter  $r$ . Other parametric values same as (26).

Figure 12 describes the influence of the treatment proportionality constant  $r$  on dynamics of model system with  $T(I) = rI$ . Figure 12, depicts that the infected population size  $I$  decreases and susceptible population  $S$  increases when treatment rate  $r$  increases with time. This suggests that the spread of disease can be decreased by increasing the treatment rate for infected population.

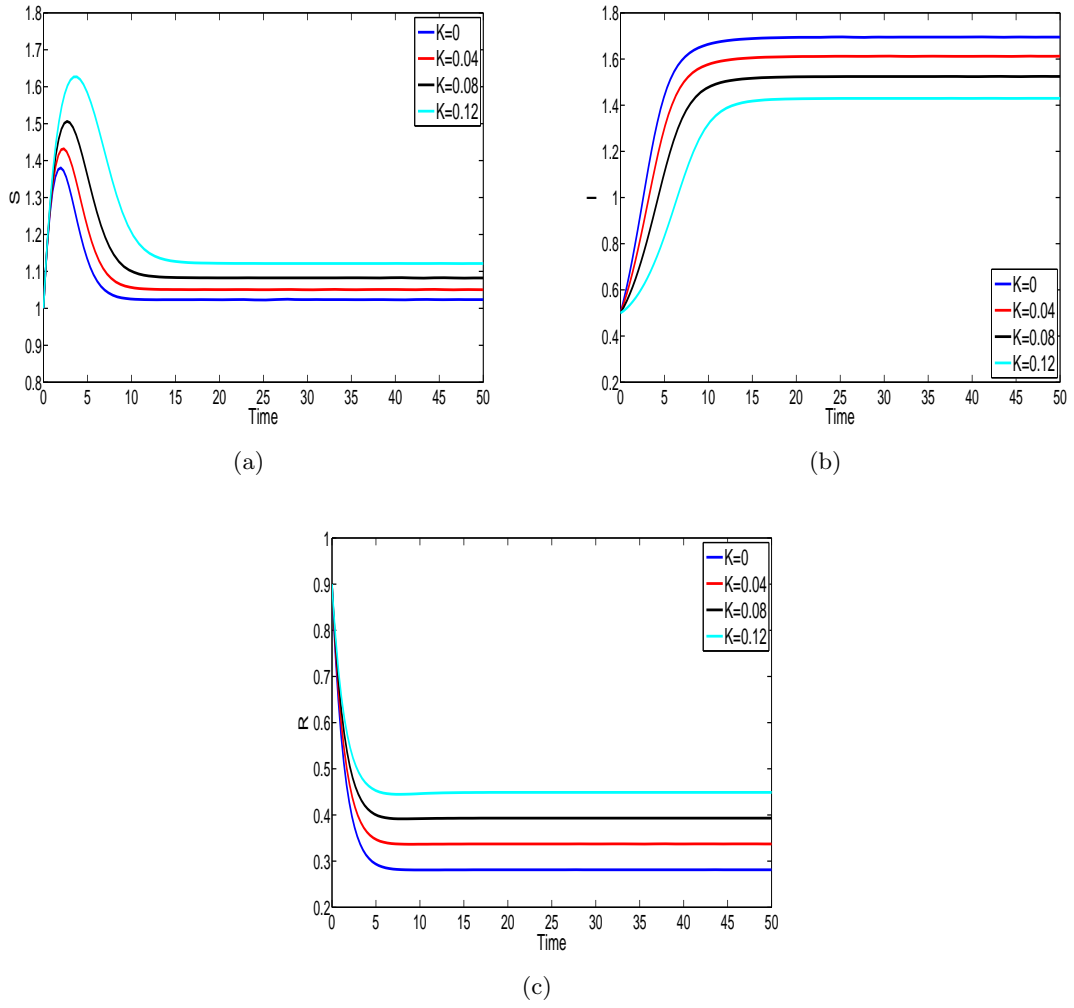
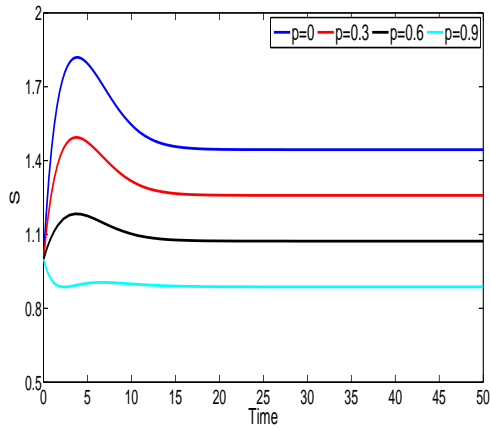
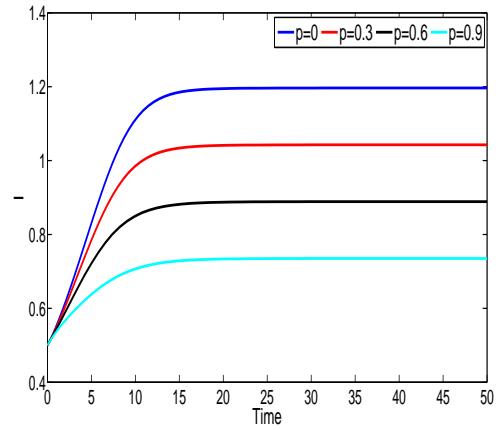


Figure 13: Dependence of  $S$ ,  $I$ , and  $R$  on the parameter  $K$ . Other parametric values are same as (26).

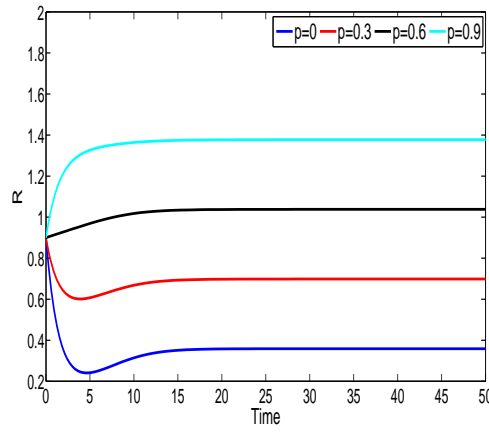
Figure 13 indicates the effect of treatment function  $T(I) = K$  on the dynamics of model system with the increasing value of  $K$ . Population size of  $S$  and  $R$  are increasing and population size of  $I$  is going down when maximal capacity of treatment  $K$  is increasing. Therefore, the constant treatment function can be used to decrease the spread of disease.



(a)



(b)



(c)

Figure 14: Dependence of  $S$ ,  $I$ , and  $R$  on the parameter  $p$ . Other parametric values are same as (26).

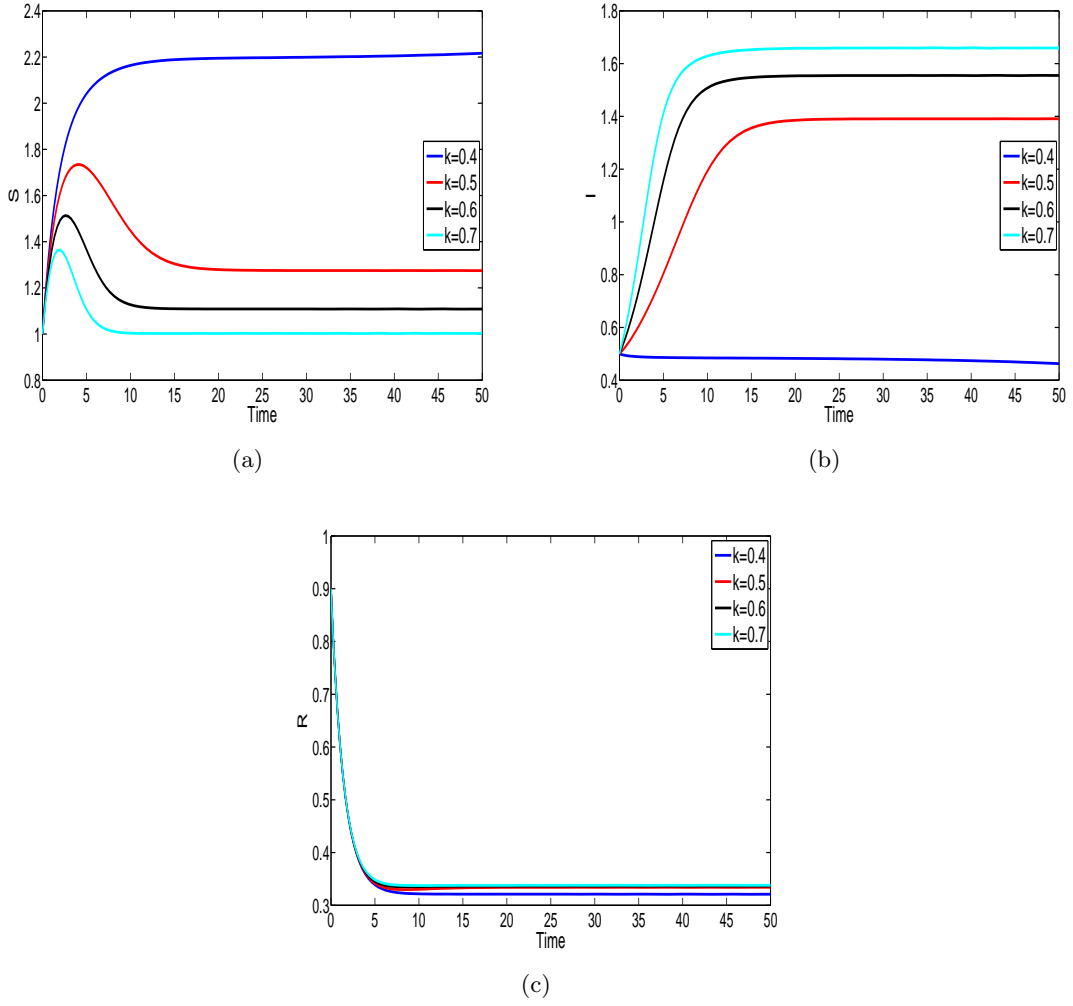


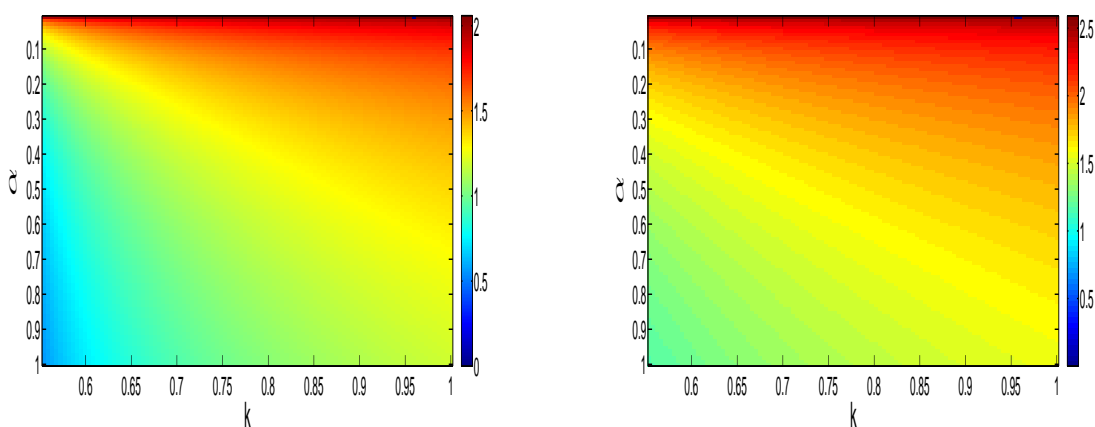
Figure 15: Dependence of  $S$ ,  $I$ , and  $R$  on the parameter  $k$ . Other parametric values are same as (26).

Figure 14 shows the effect of vaccination rate  $p$  on the populations. It is clear that size of susceptible population  $S$  and infected population  $I$  are decreasing with the increasing values of  $p$ , while the recovered population  $R$  is increasing which is expected for any type of disease. Figure 15 shows the variation of population sizes for different values of disease contact rate  $k$  with treatment function  $T(I) = K$ . Infected population size increases when disease contact rate  $k$  increases i.e. population being more infected which is evident from the Figure 15(b).

## 7.2 Effects of the infection force function

In this section, we perform the numerical simulation to explore the affect of inhibitory parameter or crowding effect on the disease for the model system (4) with both treatment functions  $T(I) = rI$  and  $T(I) = K$ . For both the cases ( $T(I) = rI$  and  $T(I) = K$ ), we assume that the infectious

force is a function of the ratio of the number of the infectives to that of the susceptibles, given by  $\frac{kIS}{S^2+\alpha I^2}$ . We perform the numerical simulation for the parametric values mentioned in (26). Figure 16(a) indicates the variation of infected population with  $T(I) = rI$  for different values of inhibitory parameter  $\alpha$  and disease contact rate  $k$ . Figure 16(b) indicates the variation of infected population with  $T(I) = K$  for different values of inhibitory parameter  $\alpha$  and disease contact rate  $k$ . In both the cases, an increase in the value of inhibitory parameter  $\alpha$ , decreases the endemic level of the disease, however, endemic level increases if the disease contact rate  $k$  increases.



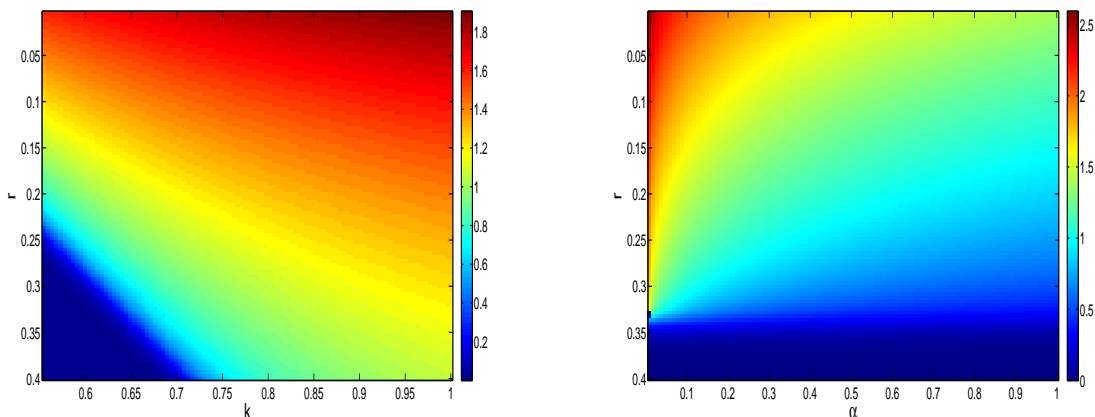
(a) The infected population with respect to various values of  $k$  and  $\alpha$ , where  $T(I) = rI$ . (b) The infected population with respect to various values of  $k$  and  $\alpha$ , where  $T(I) = K$ .

Figure 16: The Figure shows the effect of force of infection on the endemic level of the disease and the numerical value of parameters are taken from (26).

### 7.3 Effect of the treatment and infection force

Here, first we discuss the combined effect of the treatment and infection force in case of  $T(I) = rI$  (cf. Figure 17) and then the combined effect of the treatment and infection force in case of  $T(I) = K$  (cf. Figure 18). Figure 17(a) shows the endemic level of the disease for different values of treatment proportionality constant  $r$  and disease contact rate  $k$ . Infected population level decreases by increasing the treatment rate, and increases by increasing the contact rate. Figure 17(b) shows the endemic level for different values of treatment proportionality constant  $r$  and inhibitory parameter  $\alpha$ . In this Figure, we observe that infected population level decreases when inhibitory parameter  $\alpha$  and treatment proportionality constant  $r$  increase. Figure 18(a) shows the effect of maximal capacity of treatment and inhibitory parameter  $\alpha$  on the level of endemicity and concludes that infected level decreases when maximal capacity of treatment ( $K$ ) and inhibitory parameter ( $\alpha$ ) increase. Figure 18(b) shows that variation of infected population

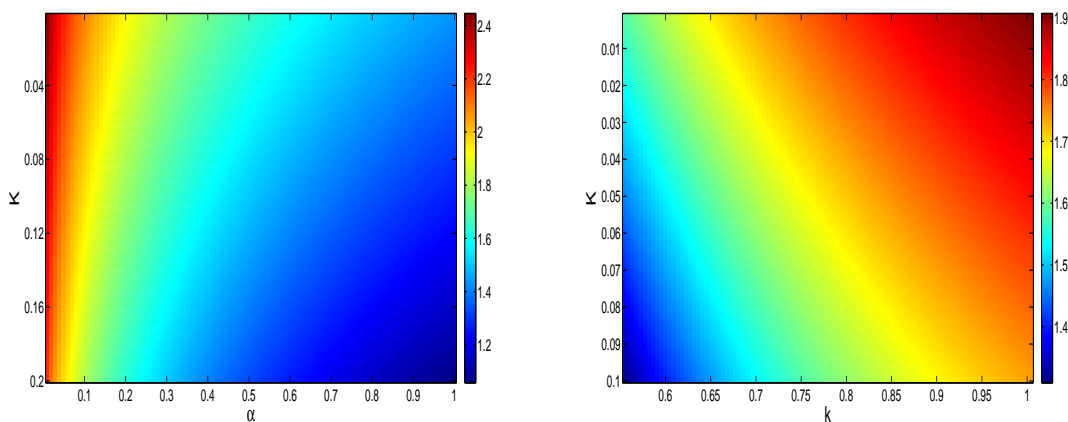
size with time for different value of  $k$  and  $K$ . We conclude that endemic level decreases when maximal capacity of treatment ( $K$ ) and increases when disease contact rate ( $k$ ) increases.



(a) The infected population level with respect to various values of  $k$  and  $r$ .

(b) The infected population level with respect to various values of  $\alpha$  and  $r$ .

Figure 17: The Figure depicts the combined effect of the treatment and infection force for  $T(I) = rI$ , where the numerical value of parameters are taken same as (26).



(a) The infected population level with respect to various values of  $\alpha$  and  $K$ .

(b) The infected population level with respect to various values of  $k$  and  $K$ .

Figure 18: The Figure depicts combined effect of the treatment and infection force for  $T(I) = K$ , where the numerical value of parameters are taken from (26).

## 8 Discussion

In the epidemiological literatures, it has been widely observed that the level of infectious individuals have a great impact on the behavioral changes of susceptible individuals, which is modeled by incidence rate. The incidence rate with a particular kind of treatment strategy significantly

influence the outbreak and spread of the concerned infectious disease.

Further, in many instances, the spread and control of infectious diseases in animals or humans could be modelled by a system of nonlinear differential equations after assuming that the population is partitioned in different classes (e.g., susceptible, infected, recovered, exposed etc.).

In particular, the SIR (Susceptible–Infected–Removed) model system provides significant theoretical and empirical basis to understand the disease mechanism in animals and humans and therefore contributing to prevention and control of infectious diseases [4]. In this work, we have proposed an SIR model system with ratio-dependent incidence rate under preventive vaccination and different treatment rates. We discussed in detail in introduction that the ratio-dependence infectious force of infection in the presence of different treatment rates might expose the complicated dynamics (bifurcations) of proposed model systems. These bifurcations along with associated bifurcations diagrams will certainly make us able to critically observe different impacts and repercussions with regard to disease spread and control.

By performing detailed stability analysis of equilibria, we have investigated the effect of various treatment functions depending on the endemic level of the disease dynamic model system (4). The impact of treatment strategies  $T(I) = rI$  and  $T(I) = K$  have been investigated extensively. We have also derived the basic reproduction number ( $\mathcal{R}_0$ ) which is influenced by parameters  $k, d, \mu, r$ . The existence of equilibria and its stability have been discussed in case of both the treatment functions. Our investigation in Section 3 assures that the model system (4) exhibits disease-free equilibrium when  $T(I) = rI$  is incorporated. Disease-free equilibrium  $E^0$  is stable if  $\mathcal{R}_0 < 1$  and saddle if  $\mathcal{R}_0 > 1$ . Further, we have derived the parametric conditions for appearance of endemic equilibria governed by the basic reproduction  $\mathcal{R}_0$ . Model system (4) does not exhibit endemic equilibria if  $\mathcal{R}_0 < 1$  and generates unique or multiple endemic equilibria when  $\mathcal{R}_0 > 1$  for  $T(I) = rI$  (refer the Theorem 3.1). The model system (4) does not exhibit any disease-free equilibrium if treatment function  $T(I) = K$ .

Further, we have investigated the impact of  $\mathcal{R}_0$  on disease dynamics which is explained in Figure 10. In Figure 10, endemicity always appear for higher impact of  $\mathcal{R}_0$  for the treatment strategy  $T(I)=K$ . The spread of disease can be controlled by increasing the maximal capacity of treatment  $I_c$ . In Figure 11, we have demonstrated the endemic level with respect to maximal capacity of treatment  $I_c$  for  $\mathcal{R}_0 < 1$  as well as  $\mathcal{R}_0 > 1$ . In Figure 11(a), when  $\mathcal{R}_0 < 1$ , endemic does not appear for the proportional treatment strategy but model system can persist disease for constant treatment strategy which can be controlled by providing the large treatment capacity. The basic reproduction number has significant impact on the disease dynamics of

model system (4). It determine whether disease persists or die out. We have demonstrated that disease appear when  $\mathcal{R}_0 > 1$  and no endemic equilibrium occurs when  $\mathcal{R}_0 < 1$  for proportional treatment strategy. But, for  $\mathcal{R}_0 < \frac{d+\mu}{d+\mu+r} < 1$ , endemicity appears when constant treatment strategy is incorporated in model system. We also investigated the sufficient conditions for global stability of unique endemic equilibrium of model system (4) using geometric approach of Li and Muldowney [48,49] in the biologically feasible region  $\Omega$ . During the course of bifurcation analysis in Section 5, we have reported that the model system (4) undergoes a saddle-node bifurcation for  $T(I)=K$ . Moreover, it is also obtained that SIR model exhibits backward bifurcation i.e., disease persists in the system even when the basic reproduction number  $\mathcal{R}_0 < 1$  at low intensity of  $I_c$  for treatment function  $T(I) = K$  (refer the Figure 11(a)). In this case, hospitals can not provide medical treatment continuously in large scale due to limitation of medical sources and capacity. Disease persists if the admitted infected populations exceed the capacity like bed, medicine and other necessary medical sources provided by hospitals. Our proposed SIR model system has multiple endemic equilibrium points when  $I_c$  lies between  $T(I) = K$  and  $T(I) = rI$  for  $\mathcal{R}_0 > 1$  (see the Figure 11(b)).

The endemic population size can be controlled/reduced by applying both the treatment strategies ( $T(I) = K$  and  $T(I) = rI$ ) as we have described in Eq. (6) that  $\mathcal{R}_0$  decreases when  $r$  increases. Theorem 3.1 and Figure 12(b) depict that disease could be disappeared by increasing the treatment rate  $r$  i.e., by enhancing the facilities related to medicine, medical equipments and other medical sources, if infected populations are below the provided capacity of treatment or availability of infected populations. In addition to this, the effects of vaccination ( $p$ ) have also been discussed on the model system (4). We obtained that the infected population size decreases by increasing vaccination rate ( $p$ ) (refer the Figure 14). From the expression of  $\mathcal{R}_0$ , it is also observed that  $\mathcal{R}_0$  increases with the increase of disease contact rate ( $k$ ) and decreases with the increase of parameters  $d$ ,  $\mu$  and  $r$ . The impact of disease contact rate ( $k$ ) on the proposed model system (4) have been discussed via Figure 15. Interestingly, from the infectious force expression, disease contact rate leaves positive effect on the infectious force i.e. more susceptible population would be transmitted into infected population which is also evident from the Figure 15.

We also discussed the impact of parameters  $K$ ,  $k$ , and  $r$  on endemic level. Level of endemicity of the model system (4) decreases with increase in maximum treatment capacity ( $K$ ). Therefore, the disease could be controlled/recovered by increasing the maximum treatment capacity. This result is evident from the Figure 13. Further, we also observe that the value of basic reproduction number ( $\mathcal{R}_0$ ) decreases with treatment rate ( $r$ ). This result shows that disease could be

controlled by increasing the treatment rate (refer the Figure 12).

We have examined the impact of different treatment functions on the dynamic model with fixing incident function (cf. Figure 12 and 13). We have also plotted the bifurcation diagrams for different treatment functions depending on endemic size which are given in Figure 10 and Figure 11.

Yuan and Li [37] proposed an SIR model system with infectious force as a function of the ratio of the number of the infectives to that of the susceptible i.e.,  $\frac{kIS}{S^2+\alpha I^2}$ . Authors found that if the natural death rate of the population and the recovery rate of infective individuals are small enough, then bistability exists; in contrast, if they are large enough, then the disease disappears. When the level of ratio of number of infective to that of susceptible is low or large enough, the infectious force increases slowly. There are some existing works [33, 37, 46, 47], with nonlinear incidence and treatment rates. However, in our work, we have considered specific ratio-dependent incidence rate, vaccination for new susceptible individuals with two different treatment rates. We clearly discussed the impacts of different significant parameters/factors (like, treatment rates, infectious force, vaccination rate, contact rate) on disease outbreak and its eradication via different bifurcations, stability and basic reproduction number. Moreover, we have made an attempt to study the comparative dynamics of existing works with our proposed SIR model system in Table 8. We hope that different dynamical behaviour discussed in this present study will provide us better insight of impacts of different treatment functions and change of human behaviours during a pandemic or epidemic threat. In turn, it we could be able to improve the disease mitigation strategies and propose the suitable health policies.

In general, in literature, we frequently come across different types of theoretical dynamics and significant computations (bifurcations, stability of equilibrium, basic reproduction number, k number etc.) of considered epidemic model system. Further, it is also very much true that the observations related to these dynamics may provide important suggestions in eradication of the concerned disease. However, it is rarely discussed that how a particular epidemic or outbreak could be described as a consequence of such a nonlinear dynamics, except, some significant attempts: refer, Hu et al. [31] for SARS outbreak in Toronto, Canada in 2003 [60], Greenhalgh and Griffiths for BSRV and Aujesky's diseases [61]. The present study may provide useful insight about the dynamics of diseases, for instance, *flu*, *measles*, *SARS*, *MERS*, and *COVID 19* in which treatment and/or change in human behaviour play significant role.

**Future Scope:** This particular study provide plenty of future works in the related area. Here, we discuss some of them specifically in three different direction: (i) Model system with

social intervention (like, media coverage and social distancing): epidemic models to an infectious disease with social distancing, quarantine, and isolation show a much more comprehensive range of dynamical behaviours with complexity. These behaviours are controlled by the various parameters which are related to social distancing, quarantine, and isolation. Here, we plan to propose and study an extension of the present epidemic model with different human intervention strategies in the homogeneous host population to control the spread of the epidemic disease. (ii) Delay induced SIR model system: In fitting the model system against the real data, we need to take into account the various types of delays between data and infection dynamics. For example, in general, confirmed cases are reported after a significant delay, which includes an incubation period and a delay between the actual test, its evaluation, and its appearance in the reported statistics. Therefore, model system with such delay effects would be an interesting realistic problem to be dealt. (iii) Model system with heterogeneities: The response of people to the introduction of different intervention strategies essentially vary among different communities and countries, which ultimately decides the impact of such public interventions. For this, heterogeneity in host population may be one of reasons. The role of heterogeneity in populations and their mobility have long been recognized as driving forces in the spread of the epidemics [63, 64]. The social contacts among the different age-group populations are also accounted by the multi-group epidemic model systems. In the case of an epidemic, generally, we observe different transmission rates in various cities and territories, depending on the cities connectivity and density of the population of a particular city. Hence, it is much clear that the heterogeneity of the host population also plays a vital role in the spread of the epidemic. Here, we plan to develop a multi-group model system by structuring the host populations into different groups according to their demographics and ages.

Existing model	Model description	Conclusion
Dongmei Xiao, Shigui Ruan [33]	Global analysis of an epidemic model with nonmonotone incidence rate	Psychological effect when the number of infectives is getting larger.
Sanling Yuan, Bo Li [37]	Global Dynamics of an epidemic model with a ratio-dependent nonlinear incidence rate	Psychological effect when the ratio of the number of infectives to that of the susceptibles is getting larger. Also studied the persistence and disappearance of disease with time.
T. K. Kar [46]	Modeling and analysis of an epidemic model with non-monotonic incidence rate under treatment	Existence and stability of equilibria are investigated for treatment strategies under non-monotonic incidence rate. Impact of maximum capacity of treatment on epidemic model.
Junhong Li, Ning Cui [47]	Dynamic behavior for an SIRS model with nonlinear incidence rate and treatment	Explored the impact of constant treatment on infected population. Model system undergoes a Hopf bifurcation and a limit cycle exists.
Our proposed study	Complicated dynamics of an SIR model with ratio-dependent incidence rate under preventive vaccination and treatment controls	<ol style="list-style-type: none"> <li>1. Treatment strategies influence the disappearance and persistence of equilibria which are described in Theorem 3.1, 3.2 and the nature of stabilities which are described in Theorem 4.2.</li> <li>2. Basic reproduction number <math>\mathcal{R}_0</math> in Eq. (6) as threshold value determine the existence and stability of equilibria in Section 3 and 4.</li> <li>3. Model system (4) exhibits backward bifurcation which is evident from Figure 10.</li> <li>4. Model system (4) undergoes a saddle-node bifurcation.</li> <li>5. We introduced some important remarks of model (4) system in Section 4.</li> <li>6. We perform the sensitivity analysis of embedding parameters of basic reproduction number <math>\mathcal{R}_0</math>. We also determine the sensitivity indices of model parameters of the endemic point of equilibrium. This investigation assure that the disease contact rate is the most sensitive parameter for susceptible level of endemic equilibrium and natural death of population is the most sensitive parameter for infected and recovered population.</li> </ol>

Table 8: Comparison of the findings of proposed SIR epidemic model system (4) with previously existing work.

## Acknowledgments

Udai Kumar's research is supported by research fellowship from MHRD, Government of India. Partha Sarathi Mandal's research is partially supported by MATRICS Project, DST, SERB, India [File No. MTR/2019/000317]. The research work of Jai Prakash Tripathi is supported by Science and Engineering Research Board (SERB), India [File No. ECR/2017/002786] and UGC-BSR Research Start-Up-Grant, India [No. F.30-356/2017(BSR)].

## A Appendix

**Lemma A.1.** (Descartes' rule of signs [51]) Let  $P(X) = \sum_{i=0}^n a_i X^i$  be a polynomial of degree  $n$  with real coefficients that has exactly  $w$  positive real roots, counted with multiplicities. Let  $v = \text{var}(a_0, a_1, \dots, a_n)$  be the number of sign variations in its coefficient sequence. Then  $v \geq w$  and  $v \equiv w \pmod{2}$ . If all the roots of  $P(X)$  are real, then  $v = w$ .

### A.1 Proof of Theorem 4.1

*Proof.* Jacobian matrix evaluated at disease-free equilibrium point  $E^0$  is given by

$$J_{E^0} = \begin{bmatrix} -d & -k & \gamma \\ 0 & k - d - \mu - r & 0 \\ 0 & \mu + r & -d - \gamma \end{bmatrix}.$$

Eigenvalues of the Jacobian matrix  $J_{E^0}$  are  $\lambda_1 = -d$ ,  $\lambda_2 = k - d - \mu - r$  and  $\lambda_3 = -d - \gamma$ . Clearly eigenvalues  $\lambda_1, \lambda_2$  are negative due to positiveness of parameter  $d$  and  $\gamma$ . Here,  $\lambda_3 = (d + \mu + r)(\mathcal{R}_0 - 1)$ . Clearly eigenvalue  $\lambda_3$  is negative if  $\mathcal{R}_0 < 1$ .  $\square$

### A.2 Proof of Theorem 4.2

*Proof.* The Jacobian matrix for the model system (4) is given by

$$J = \begin{bmatrix} -d - \frac{2\alpha k S I^3}{(S^2 + \alpha I^2)^2} & -\frac{k S^2 (S^2 - \alpha I^2)}{(S^2 + \alpha I^2)^2} & \gamma \\ \frac{2\alpha k S I^3}{(S^2 + \alpha I^2)^2} & \frac{k S^2 (S^2 - \alpha I^2)}{(S^2 + \alpha I^2)^2} - d - \mu - T'(I) & 0 \\ 0 & \mu + T'(I) & -d - \gamma \end{bmatrix}. \quad (\text{A.1})$$

Characteristic equation at endemic equilibrium  $E^* = (S^*, I^*, R^*)$  is given by  $\lambda^3 + \sigma_1 \lambda^2 + \sigma_2 \lambda + \sigma_3 = 0$ , where

$$\begin{aligned} \sigma_1 &= 3d + \frac{2\alpha k S I^3}{(S^2 + \alpha I^2)^2} + \frac{k S^2 (\alpha I^2 - S^2)}{(S^2 + \alpha I^2)^2} + \mu + T'(I) + \gamma, \\ \sigma_2 &= \left[ \frac{k S^2 (\alpha I^2 - S^2)}{(S^2 + \alpha I^2)^2} \right] [2d + \mu] + \left[ d + \frac{2\alpha k S I^3}{(S^2 + \alpha I^2)^2} \right] [2d + \mu + \gamma + T'] + [d + \mu + T'] [d + \gamma], \\ \sigma_3 &= d(d + \gamma) \left[ \frac{k S^2 (\alpha I^2 - S^2)}{(S^2 + \alpha I^2)^2} + d + \mu + T' \right] + \frac{2\alpha k S I^3}{(S^2 + \alpha I^2)^2} [d(d + \mu + T') + \gamma d]. \end{aligned} \quad (\text{A.2})$$

After a little algebraic calculation, we obtain

$$\begin{aligned}
\sigma_1\sigma_2 - \sigma_3 &= \left[3d + \frac{2\alpha kSI^3}{(S^2 + \alpha I^2)^2} + \frac{kS^2(\alpha I^2 - S^2)}{(S^2 + \alpha I^2)^2} + \mu + T'(I) + \gamma\right] \left[\left(\frac{2\alpha kSI^3}{(S^2 + \alpha I^2)^2}\gamma + (\mu + T')(d + \gamma)\right)\right] \\
&\quad + d(d + \gamma) \left[2d + \frac{2\alpha kSI^3}{(S^2 + \alpha I^2)^2} + \gamma\right] + d\gamma \left[3d + \frac{kS^2(\alpha I^2 - S^2)}{(S^2 + \alpha I^2)^2} + \mu + T'(I) + \gamma\right], \\
&\quad + \frac{2\alpha kSI^3}{(S^2 + \alpha I^2)^2} (d + \mu + T') \left[2d + \frac{2\alpha kSI^3}{(S^2 + \alpha I^2)^2} + \frac{kS^2(\alpha I^2 - S^2)}{(S^2 + \alpha I^2)^2} + \mu + T'(I) + \gamma\right]. \quad (\text{A.3})
\end{aligned}$$

Furthermore, the stability properties of different equilibria of model system (4) with both the treatment functions (for the parameter value (26)) have been demonstrated in Table 4.

### A.3 Proof of Theorem 4.3

We obtained that for the treatment rate  $T(I)$ , the disease-free equilibrium  $E^0 = (S^0, 0, R^0)$  of model system (4) is locally asymptotically stable whenever  $\mathcal{R}_0 < 1$ . We apply comparison principal [58] to show that  $I(t) \rightarrow 0$  as  $t \rightarrow \infty$  when  $\mathcal{R}_0 < 1$ . Since  $(S, I, R) \in \mathbb{R}_+^3$ , from the second equation of model system (4), we observe that

$$\frac{dI}{dt} = \frac{kIS^2}{(S^2 + \alpha I^2)} - (d + \mu + r)I < (d + \mu + r)(\mathcal{R}_0 - 1)I. \quad (\text{A.4})$$

The linear comparison model of (A.4) is given by

$$\frac{d\hat{I}}{dt} = (d + \mu + r)(\mathcal{R}_0 - 1)\hat{I}, \quad \hat{I}(0) = I(0). \quad (\text{A.5})$$

If  $\mathcal{R}_0 < 1$ ,  $\hat{I}(t) \rightarrow 0$  as  $t \rightarrow \infty$ . By comparison principal,  $I(t) \rightarrow 0$  as  $t \rightarrow \infty$ . Hence, for any small  $\varepsilon > 0$ , there exists  $t_0 > 0$  such that for all  $t \geq t_0$ ,  $I(t) \leq \varepsilon$ . From the third equation of model system (4), we obtain

$$\frac{dR}{dt} = pb + \mu I - (d + \gamma)R + rI < pb + (\mu + r)\varepsilon - (d + \gamma)R. \quad (\text{A.6})$$

The linear comparison model of (A.6) is given by

$$\frac{d\hat{R}}{dt} = pb + (\mu + r)\varepsilon - (d + \gamma)\hat{R}, \quad \hat{R}(0) = R(0), \quad t \geq t_0. \quad (\text{A.7})$$

From Eq. (A.7), we have  $\hat{R}(t) \rightarrow \frac{pb}{d+\gamma}$  as  $t \rightarrow \infty$ . Using the comparison principal [58], we obtain  $R(t) \rightarrow \frac{pb}{d+\gamma}$  as  $t \rightarrow \infty$ . Hence, for any small  $\varepsilon > 0$  and  $t \geq t_0$ , we obtain  $R(t) \leq \frac{pb}{d+\gamma} + \varepsilon$ . From the first equation of model system (4), we obtain

$$\frac{dS}{dt} = (1 - p)b - dS - \frac{kIS^2}{S^2 + \alpha I^2} + \gamma R < (1 - p)b - dS + \gamma \left(\frac{pb}{d + \gamma} + \varepsilon\right). \quad (\text{A.8})$$

The linear comparison model of (A.8) is given by

$$\frac{d\hat{S}}{dt} = (1-p)b - d\hat{S} + \gamma\left(\frac{pb}{d+\gamma} + \varepsilon\right), \quad \hat{S}(0) = S(0). \quad (\text{A.9})$$

From Eq. (A.9),  $\hat{S}(t) \rightarrow \frac{1}{d}(1-p)b + \frac{\gamma pb}{d+\gamma}$  as  $t \rightarrow \infty$ . Using the comparison principal, we obtain  $S(t) \leq \frac{1}{d}(1-p)b + \frac{\gamma pb}{d+\gamma}$ . Hence, for any small  $\varepsilon > 0$ , and  $t \geq t_0$ , we obtain  $S(t) \leq \frac{1}{d}(1-p)b + \frac{\gamma pb}{d+\gamma} + \varepsilon$ . Therefore, the disease-free equilibrium  $E^0 = (S^0, 0, R^0)$  is globally asymptotic stable if  $\mathcal{R}_0 < 1$ .

#### A.4 Proof of Theorem 4.4

We apply the geometric approach method of Li and Muldowney [48, 49] to study the global stability of an endemic  $E^* = (S^*, I^*, R^*)$  of model system (4) in the feasible region  $\Omega$ . Let the map  $x \rightarrow f(x)$  be a  $C^1$  function from an open and simply connected subset  $\Omega \subset \mathbb{R}^n$  to  $\mathbb{R}^n$  and  $x(t)$  is the solution of the following differential equation

$$\dot{x} = f(x). \quad (\text{A.10})$$

Each solution  $x(t)$  of Eq. (A.10) is uniquely determined by its initial value  $x(0) = x_0$  and denoted by  $x(t, x_0)$ . We formulate the problem with the following assumptions:

H1: There is a compact absorbing set  $\Gamma \subset \Omega$ .

H2: Eq. (A.10) has a unique equilibrium  $x^*$  in  $\Omega$ .

We find condition under which the global stability of  $x^*$  with respect to  $\Omega$  is implied by its local stability [49].

Consider a nonsingular  $\binom{n}{2} \times \binom{n}{2}$  matrix valued function  $x \rightarrow A(x)$  which is  $C^1$  class in  $\Omega$ . Under the assumptions H1 and H2, if  $A^{-1}(x)$  exists and is continuous for  $x \in \Gamma$ , the set

$$Z = A_f A^{-1} + A \frac{\partial f^{[2]}}{\partial x} A^{-1}, \quad (\text{A.11})$$

where, the matrix  $A_f$  is the matrix obtained by replacing each  $a_{ij}$  in  $A$  by its directional derivative in the direction of  $f$  and is defined as

$$(a_{ij})_f = \left(\frac{da_{ij}}{dx}\right)^T \cdot f(x) = \Delta a_{ij} \cdot f(x),$$

$\frac{\partial f^{[2]}}{\partial x}$  is the second additive compound matrix of the Jacobian matrix  $\frac{\partial f}{\partial x}$  of  $f$ . Thus, define a quantity  $Q$  by

$$Q = \lim_{x \rightarrow \infty} \sup_{x_0 \in \Gamma} \frac{1}{t} \int_0^t \omega(Z(x(s, x_0))) ds, \quad (\text{A.12})$$

where  $\omega(Z)$  is the Lozinskii measure [49] of  $Z$  is defined by

$$\omega(Z) = \lim_{\theta \rightarrow 0^+} \frac{|\mathcal{I} + \theta Z| - 1}{\theta},$$

where  $\mathcal{I}$  is the identity matrix of the same dimension as  $Z$ ,  $\theta$  is a real positive number and  $|\cdot|$  is the induced matrix norm.

**Lemma A.2.** *Under the assumptions (H1) and (H2), the unique equilibrium  $x^*$  of model system (A.10) is globally asymptotically stable in  $\Omega$  if there exists a function  $A(x)$  and the Lozinskii measure  $\omega$  such that  $Q < 0$ .*

*Proof.* Under the condition provided in Theorem (3.1), model system (4) has a unique endemic equilibrium  $E^* = (S^*, I^*, R^*)$  in the interior of  $\Omega$ . Thus model system (4) satisfies assumption (H2). From [48, 49], it is easy to observe that the model system (4) is uniformly persistent i.e., there is a constant  $\epsilon > 0$  such that every solution  $(S(t), I(t), R(t))$  of model system (4) with initial value  $(S(0), I(0), R(0))$  in the interior of  $\Omega$  is given by (5), and satisfy

$$\liminf_{t \rightarrow \infty} |(S(t), I(t), R(t))| \geq \epsilon.$$

It shows the existence of a compact set  $\Gamma$  which is absorbing set in the interior of  $\Omega$ . This also verifies the assumption H1. The second additive compound matrix for the Jacobian matrix of model system (4) at  $E^*$  is given by

$$J^{[2]} = \frac{\partial f^{[2]}}{\partial x} = \begin{bmatrix} -2d - \frac{2\alpha k S I^3}{(S^2 + \alpha I^2)^2} + \frac{k\alpha S^2(S^2 - \alpha I^2)}{(S^2 + \alpha I^2)^2} - \mu - r & 0 & -\gamma \\ \mu + r & \frac{2\alpha k S I^3(S^2 - \alpha I^2)}{(S^2 + \alpha I^2)^2} - 2d - \gamma & -\frac{k S^2(S^2 - \alpha I^2)}{(S^2 + \alpha I^2)^2} \\ 0 & \frac{2\alpha k S I^3}{(S^2 + \alpha I^2)^2} & \frac{k S^2(S^2 - \alpha I^2)}{(S^2 + \alpha I^2)^2} - 2d - \mu - r - \gamma \end{bmatrix}.$$

Choose a compound matrix  $A$  by  $A = \frac{1}{I} \mathcal{I}_3$  and

$$A_f A^{-1} = -\frac{1}{I} \frac{dI}{dt} \mathcal{I}_3 \text{ and } Z = A_f A^{-1} + A J^{[2]} A^{-1} = \begin{bmatrix} Z_{11} & Z_{12} \\ Z_{21} & Z_{22} \end{bmatrix}. \text{ where } Z_{11} = -d - \frac{2\alpha k S I^3}{(S^2 + \alpha I^2)^2} + \frac{k\alpha S^2(S^2 - \alpha I^2)}{(S^2 + \alpha I^2)^2} - \frac{k S^2}{(S^2 + \alpha I^2)^2}, Z_{12} = (0, -\gamma), Z_{21} = \mu + r \text{ and}$$

$$Z_{22} = \begin{bmatrix} \mu + r - d - \gamma - \frac{k S^2}{(S^2 + \alpha I^2)^2} - \frac{2\alpha k S I^3}{(S^2 + \alpha I^2)^2} & -\frac{k S^2(S^2 - \alpha I^2)^2}{(S^2 + \alpha I^2)^2} \\ \frac{2\alpha k S I^3}{(S^2 + \alpha I^2)^2} & -\frac{k S^2}{(S^2 + \alpha I^2)^2} + \frac{k S^2(S^2 - \alpha I^2)^2}{(S^2 + \alpha I^2)^2} - d - \gamma \end{bmatrix}.$$

Let the vector norm in  $\mathbb{R}^3$  is given by

$$|(x_1, x_2, x_3)| = \max\{|x_1|, |x_2| + |x_3|\}. \quad (\text{A.13})$$

Lozinskii measure  $\omega(Z)$  with respect to  $|\cdot|$  can be estimated as

$$\omega(Z) \leq \sup\{g_1, g_2\} = \sup\{\omega(Z_{11}) + |Z_{12}|, \omega(Z_{22}) + |Z_{21}|\},$$

where  $|Z_{12}|$ ,  $|Z_{21}|$  are the matrix norms with respect to  $\omega$  norm. Hence we obtain

$$\begin{aligned}
g_1 &= \omega(Z_{11}) + |Z_{12}| = -d - \frac{2\alpha k S I^3}{(S^2 + \alpha I^2)^2} + \frac{k\alpha S^2(S^2 - \alpha I^2)}{(S^2 + \alpha I^2)^2} - \frac{kS^2}{(S^2 + \alpha I^2)^2} + \gamma + k\alpha \\
&\leq -\left(d + \frac{kS^2}{(S^2 + \alpha I^2)^2}\right) + \gamma + k\alpha \\
&\leq -\frac{I'}{I} + \gamma - 2d - \mu - r + k\alpha \\
&\leq -\frac{I'}{I} - (2d + \mu + r - \gamma - k\alpha),
\end{aligned}$$

$$\begin{aligned}
g_2 &= \omega(Z_{22}) + |Z_{21}| \\
&= \max\left\{\mu + r - \left(d + \gamma + \frac{kS^2}{(S^2 + \alpha I^2)^2}\right), -\left(\frac{kS^2}{(S^2 + \alpha I^2)^2} + \frac{kS^2(S^2 - \alpha I^2)^2}{(S^2 + \alpha I^2)^2} + d + \gamma\right)\right\} + \mu + r \\
&\leq -\frac{I'}{I} - (d + \gamma - \mu - r - k\alpha).
\end{aligned} \tag{A.14}$$

Therefore,

$$\omega(Z) \leq \sup\{g_1, g_2\} = -\frac{I'}{I} - \min\{(2d + \mu + r - \gamma - k\alpha), (d + \gamma - \mu - r - k\alpha)\},$$

which holds along any solution  $(S(t), I(t), R(t))$  of model system (4) with  $(S(0), I(0), R(0)) \in \Omega$ , where  $\Omega$  is the compact absorbing set. Thus, we have,

$$\frac{1}{t} \int_0^t \omega(Z) dI \leq \frac{1}{t} \log \frac{I(0)}{I(t)} - c,$$

by taking limit as  $t \rightarrow \infty$ , we get

$$Q = \lim_{t \rightarrow \infty} \sup \sup \frac{1}{t} \int_0^t \omega(Z) dI \leq -\frac{c}{2} < 0.$$

From Lemma A.2, it implies that  $E^* = (S^*, I^*, R^*)$  is globally asymptotically stable in the interior of  $\Omega$ . This completes the proof.  $\square$

## A.5 Sensitivity indices

For the parameters value given in (26) model (5) has stable endemic equilibrium

$E^*(1.320622933, 1.094026316, 0.5853507518)$ . Matrix A is Jacobian matrix  $J_{E^*}$  which is given by as follows:

$$A = \begin{bmatrix} -0.4819968139 & -0.2903076924 & 0.4 \\ 0.1819968138 & -0.2196923076 & 0 \\ 0 & 0.21 & -0.7 \end{bmatrix} \tag{A.15}$$

In order to find the solution of linear system (29), we have to calculate the vector  $K_j$  for  $j=1,2,\dots,8$ .

### Sensitivity index of p

For j=1, vector  $K_1$  can be obtain as follows:

$$K_1 = \begin{bmatrix} -y_1 \\ 0 \\ y_1 \end{bmatrix} = \begin{bmatrix} -0.9 \\ 0 \\ 0.9 \end{bmatrix} \quad (\text{A.16})$$

Now, using (A.16) and (A.15) in (29), we get solution vector

$$X_1 = \begin{bmatrix} \frac{\partial s_1^*}{\partial y_1} \\ \frac{\partial s_2^*}{\partial y_1} \\ \frac{\partial s_3^*}{\partial y_1} \end{bmatrix} = \begin{bmatrix} -0.6190419994 \\ -0.5128248355 \\ 1.131866835 \end{bmatrix} \quad (\text{A.17})$$

Sensitivity index of p is obtained as follows:

$$\begin{aligned} \gamma_p^{s_1^*} &= \frac{\partial s_1^*}{\partial y_1} \cdot \frac{y_1}{s_1^*} = [-0.6190419994] \left[ \frac{0.2}{1.320622933} \right] = -0.09374999995. \\ \gamma_p^{s_2^*} &= \frac{\partial s_2^*}{\partial y_1} \cdot \frac{y_1}{s_2^*} = [-0.5128248355] \left[ \frac{0.2}{1.094026316} \right] = -0.09374999998. \\ \gamma_p^{s_3^*} &= \frac{\partial s_3^*}{\partial y_1} \cdot \frac{y_1}{s_3^*} = [1.131866835] \left[ \frac{0.2}{0.5853507518} \right] = 0.3867311460. \end{aligned} \quad (\text{A.18})$$

### Sensitivity index of b

For j=2, vector  $K_2$  can be obtain as follows:

$$K_2 = \begin{bmatrix} 1 - y_1 \\ 0 \\ y_1 \end{bmatrix} = \begin{bmatrix} 0.8 \\ 0 \\ 0.2 \end{bmatrix} \quad (\text{A.19})$$

Now, using (A.19) and (A.15) in (29), we get solution vector

$$X_2 = \begin{bmatrix} \frac{\partial s_1^*}{\partial y_2} \\ \frac{\partial s_2^*}{\partial y_2} \\ \frac{\partial s_3^*}{\partial y_2} \end{bmatrix} = \begin{bmatrix} 1.467358813 \\ 1.215584795 \\ 0.6503897243 \end{bmatrix} \quad (\text{A.20})$$

Sensitivity index of b is obtained as follows:

$$\begin{aligned} \gamma_b^{s_1^*} &= \frac{\partial s_1^*}{\partial y_2} \cdot \frac{y_2}{s_1^*} = [1.467358813] \left[ \frac{0.9}{1.320622933} \right] = 0.9999999990. \\ \gamma_b^{s_2^*} &= \frac{\partial s_2^*}{\partial y_2} \cdot \frac{y_2}{s_2^*} = [1.215584795] \left[ \frac{0.9}{1.094026316} \right] = 0.9999999995. \\ \gamma_b^{s_3^*} &= \frac{\partial s_3^*}{\partial y_2} \cdot \frac{y_2}{s_3^*} = [0.6503897243] \left[ \frac{0.9}{0.5853507518} \right] = 1. \end{aligned} \quad (\text{A.21})$$

### Sensitivity index of d

For j=3, vector  $K_3$  can be obtain as follows:

$$K_3 = \begin{bmatrix} -s_1^* \\ -s_2^* \\ -s_3^* \end{bmatrix} = \begin{bmatrix} -1.320622933 \\ -1.094026316 \\ -0.5853507518 \end{bmatrix} \quad (\text{A.22})$$

Now, using (A.22) and (A.15) in (29), we get solution vector

$$X_3 = \begin{bmatrix} \frac{\partial s_1^*}{\partial y_3} \\ \frac{\partial s_2^*}{\partial y_3} \\ \frac{\partial s_3^*}{\partial y_3} \end{bmatrix} = \begin{bmatrix} -1.295187621 \\ -6.05276694 \\ -2.652045442 \end{bmatrix} \quad (\text{A.23})$$

Sensitivity index of d is obtained as follows:

$$\begin{aligned} \gamma_d^{s_1^*} &= \frac{\partial s_1^*}{\partial y_3} \cdot \frac{y_3}{s_1^*} = [-1.295187621] \left[ \frac{0.3}{1.320622933} \right] = -0.2942219741. \\ \gamma_d^{s_2^*} &= \frac{\partial s_2^*}{\partial y_3} \cdot \frac{y_3}{s_2^*} = [-6.05276694] \left[ \frac{0.3}{1.094026316} \right] = -1.659768193. \\ \gamma_d^{s_3^*} &= \frac{\partial s_2^*}{\partial y_3} \cdot \frac{y_3}{s_2^*} = [-2.652045442] \left[ \frac{0.3}{0.5853507518} \right] = -1.359208355. \end{aligned}$$

### Sensitivity index of k

Taking j=4, vector  $K_4$  is given by as follows:

$$K_4 = \begin{bmatrix} -\frac{s_1^{*2} s_2^*}{s_1^{*2} + y_5 s_2^{*2}} \\ \frac{s_1^{*2} s_2^*}{s_1^{*2} + y_5 s_2^{*2}} \\ 0 \end{bmatrix} = \begin{bmatrix} -0.8583898788 \\ 0.8583898788 \\ 0 \end{bmatrix} \quad (\text{A.24})$$

Now, using (A.24) and (A.15) in (29), we get solution vector

$$X_4 = \begin{bmatrix} \frac{\partial s_1^*}{\partial y_4} \\ \frac{\partial s_2^*}{\partial y_4} \\ \frac{\partial s_3^*}{\partial y_4} \end{bmatrix} = \begin{bmatrix} -2.445618639 \\ 1.881245107 \\ 0.5643735322 \end{bmatrix} \quad (\text{A.25})$$

Sensitivity index of k is obtained as follows:

$$\begin{aligned} \gamma_k^{s_1^*} &= \frac{\partial s_1^*}{\partial y_4} \cdot \frac{y_4}{s_1^*} = [-2.445618639] \left[ \frac{0.65}{1.320622933} \right] = -1.20371385. \\ \gamma_k^{s_2^*} &= \frac{\partial s_2^*}{\partial y_4} \cdot \frac{y_4}{s_2^*} = [1.881245107] \left[ \frac{0.65}{1.094026316} \right] = 1.117714722. \\ \gamma_k^{s_3^*} &= \frac{\partial s_2^*}{\partial y_4} \cdot \frac{y_4}{s_2^*} = [0.5643735322] \left[ \frac{0.65}{0.5853507518} \right] = 0.6267059447. \end{aligned}$$

### Sensitivity index of $\alpha$

For j=5, vector  $K_5$  takes the following form:

$$K_5 = \begin{bmatrix} \frac{y_4 s_1^{*2} s_2^{*3}}{(s_1^{*2} + y_5 s_2^{*2})^2} \\ -\frac{y_4 s_1^{*2} s_2^{*3}}{(s_1^{*2} + y_5 s_2^{*2})^2} \\ 0 \end{bmatrix} = \begin{bmatrix} 0.3004364576 \\ -0.3004364576 \\ 0 \end{bmatrix} \quad (\text{A.26})$$

Now, using (A.26) and (A.15) in (29), we get solution vector

$$X_5 = \begin{bmatrix} \frac{\partial s_1^*}{\partial y_5} \\ \frac{\partial s_2^*}{\partial y_5} \\ \frac{\partial s_3^*}{\partial y_5} \end{bmatrix} = \begin{bmatrix} 0.8559665236 \\ -0.6584357876 \\ -1.975307363 \end{bmatrix} \quad (\text{A.27})$$

Sensitivity index of  $\alpha$  is obtained as follows:

$$\begin{aligned}\gamma_{\alpha}^{s_1^*} &= \frac{\partial s_1^*}{\partial y_5} \cdot \frac{y_5}{s_1^*} = [0.8559665236] \left[ \frac{0.4}{1.320622933} \right] = 0.2592614446. \\ \gamma_{\alpha}^{s_2^*} &= \frac{\partial s_2^*}{\partial y_5} \cdot \frac{y_5}{s_2^*} = [-0.6584357876] \left[ \frac{0.4}{1.094026316} \right] = -0.2407385555. \\ \gamma_{\alpha}^{s_3^*} &= \frac{\partial s_3^*}{\partial y_5} \cdot \frac{y_5}{s_2^*} = [-0.1975307363] \left[ \frac{0.4}{0.5853507518} \right] = -0.1349828189.\end{aligned}$$

### Sensitivity index of $\gamma$

For  $j=6$ , vector  $K_6$  can be determined as follows:

$$K_6 = \begin{bmatrix} s_3^* \\ 0 \\ -s_3^* \end{bmatrix} = \begin{bmatrix} 0.5853507518 \\ 0 \\ -0.5853507518 \end{bmatrix} \quad (\text{A.28})$$

Now, using (A.28) and (A.15) in (29), we get solution vector

$$X_6 = \begin{bmatrix} \frac{\partial s_1^*}{\partial y_6} \\ \frac{\partial s_2^*}{\partial y_6} \\ \frac{\partial s_3^*}{\partial y_6} \end{bmatrix} = \begin{bmatrix} 0.4026185553 \\ 0.3335360033 \\ -0.7361545587 \end{bmatrix} \quad (\text{A.29})$$

Sensitivity index of  $\gamma$  is obtained as follows:

$$\begin{aligned}\gamma_{\gamma}^{s_1^*} &= \frac{\partial s_1^*}{\partial y_6} \cdot \frac{y_6}{s_1^*} = [0.4026185553] \left[ \frac{0.4}{1.3206229332} \right] = 0.1219480732. \\ \gamma_{\gamma}^{s_2^*} &= \frac{\partial s_2^*}{\partial y_6} \cdot \frac{y_6}{s_2^*} = [0.3335360033] \left[ \frac{0.4}{1.094026316} \right] = 0.1219480732. \\ \gamma_{\gamma}^{s_3^*} &= \frac{\partial s_3^*}{\partial y_6} \cdot \frac{y_6}{s_2^*} = [-0.7361545587] \left[ \frac{0.4}{0.5853507518} \right] = -0.5030519267.\end{aligned} \quad (\text{A.30})$$

### Sensitivity index of $\mu$

For  $j=7$ , vector  $K_7$  can be obtained as follows:

$$K_7 = \begin{bmatrix} 0 \\ -s_2^* \\ s_2^* \end{bmatrix} = \begin{bmatrix} 0 \\ -1.094026316 \\ 1.094026316 \end{bmatrix} \quad (\text{A.31})$$

Now, using (A.31) and (A.15) in (29), we get solution vector

$$X_7 = \begin{bmatrix} \frac{\partial s_1^*}{\partial y_7} \\ \frac{\partial s_2^*}{\partial y_7} \\ \frac{\partial s_3^*}{\partial y_7} \end{bmatrix} = \begin{bmatrix} 2.364466889 \\ -3.021047405 \\ 0.6565805155 \end{bmatrix} \quad (\text{A.32})$$

Sensitivity index of  $\mu$  is obtained as follows:

$$\begin{aligned}\gamma_{\mu}^{s_1^*} &= \frac{\partial s_1^*}{\partial y_7} \cdot \frac{y_7}{s_1^*} = [2.364466889] \left[ \frac{0.01}{1.320622933} \right] = 0.01790417863. \\ \gamma_{\mu}^{s_2^*} &= \frac{\partial s_2^*}{\partial y_7} \cdot \frac{y_7}{s_2^*} = [-3.021047405] \left[ \frac{0.01}{1.094026316} \right] = -0.02761402866. \\ \gamma_{\mu}^{s_3^*} &= \frac{\partial s_3^*}{\partial y_7} \cdot \frac{y_7}{s_2^*} = [0.6565805155] \left[ \frac{0.01}{0.5853507518} \right] = 0.01121687319.\end{aligned}$$

### Sensitivity index of $r$

For  $j=8$ , vector  $K_8$  can be obtained as follows:

$$K_8 = \begin{bmatrix} 0 \\ -s_2^* \\ s_2^* \end{bmatrix} = \begin{bmatrix} 0 \\ -1.094026316 \\ 1.094026316 \end{bmatrix} \quad (\text{A.33})$$

Now, using (A.33) and (A.15) in (29), we get solution vector

$$X_8 = \begin{bmatrix} \frac{\partial s_1^*}{\partial y_8} \\ \frac{\partial s_2^*}{\partial y_8} \\ \frac{\partial s_3^*}{\partial y_8} \end{bmatrix} = \begin{bmatrix} 2.364466889 \\ -3.021047405 \\ 0.6565805155 \end{bmatrix} \quad (\text{A.34})$$

Sensitivity index of  $r$  is obtained as follows:

$$\begin{aligned} \gamma_r^{s_1^*} &= \frac{\partial s_1^*}{\partial y_8} \cdot \frac{y_8}{s_1^*} = [2.364466889] \left[ \frac{0.2}{1.320622933} \right] = 0.3580835726. \\ \gamma_r^{s_2^*} &= \frac{\partial s_2^*}{\partial y_8} \cdot \frac{y_8}{s_2^*} = [-3.021047405] \left[ \frac{0.2}{1.094026316} \right] = -0.5522805733. \\ \gamma_r^{s_3^*} &= \frac{\partial s_3^*}{\partial y_8} \cdot \frac{y_8}{s_2^*} = [0.6565805155] \left[ \frac{0.2}{0.5853507518} \right] = 0.2243374638. \end{aligned}$$

## References

- [1] World Health Organization, [https://www.who.int/whr/1996/media\\_centre/press\\_release/en/](https://www.who.int/whr/1996/media_centre/press_release/en/).
- [2] Yang Y, Xiao D, Influence of latent period and nonlinear incidence rate on the dynamics of SIRS epidemiological models, *Discrete & Continuous Dynamical Systems-B*, 13(1) (2010): 195.
- [3] Hethcote HW, The mathematics of infectious diseases. *SIAM Review*, 42(4) (2000): 599-653.
- [4] Anderson RM, Anderson B, May RM, *Infectious diseases of humans: dynamics and control*, Oxford university press, (1992).
- [5] Diekmann O, Heesterbeek JA, Metz JA, On the definition and the computation of the basic reproduction ratio  $R_0$  in models for infectious diseases in heterogeneous populations, *Journal of Mathematical Biology*, 28(4) (1990): 365-382.
- [6] Li J, Zhou Y, Wu J, Ma Z, Complex dynamics of a simple epidemic model with a nonlinear incidence, *Discrete & Continuous Dynamical Systems-B*, 8(1) (2007): 161.

- [7] Huang G, Takeuchi Y, Ma W, Wei D, Global stability for delay SIR and SEIR epidemic models with nonlinear incidence rate, *Bulletin of Mathematical Biology*, 72(5) (2010): 1192-1207.
- [8] Ruan S, Wang W, Dynamical behavior of an epidemic model with a nonlinear incidence rate, *Journal of Differential Equations*, 188(1) (2003): 135-163.
- [9] Alexander ME, Moghadas SM, Bifurcation analysis of an SIRS epidemic model with generalized incidence, *SIAM Journal on Applied Mathematics*, 65(5) (2005): 1794-1816.
- [10] Van den Driessche P, Watmough J, Reproduction numbers and sub-threshold endemic equilibria for compartmental models of disease transmission, *Mathematical Biosciences*, 180(1-2) (2002): 29-48.
- [11] Korobeinikov A, Maini PK, Walker WJ, Estimation of effective vaccination rate: pertussis in New Zealand as a case study, *Journal of Theoretical Biology*, 224(2) (2003): 269-275.
- [12] Hu Z, Bi P, Ma W, Ruan S, Bifurcations of an SIRS epidemic model with nonlinear incidence rate, *Discrete & Continuous Dynamical Systems-B*, 15(1) (2011): 93.
- [13] Tang Y, Huang D, Ruan S, Zhang W, Coexistence of limit cycles and homoclinic loops in a SIRS model with a nonlinear incidence rate, *SIAM Journal on Applied Mathematics*, 69(2) (2008): 621-639.
- [14] Cui J, Sun Y, Zhu H, The impact of media on the control of infectious diseases, *Journal of Dynamics and Differential Equations*, 20(1) (2008): 31-53.
- [15] Wang W, Epidemic models with nonlinear infection forces, *Mathematical Biosciences & Engineering*, 3(1) (2006): 267.
- [16] Wu LI, Feng Z, Homoclinic bifurcation in an SIQR model for childhood diseases, *Journal of Differential Equations*, 168(1) (2000): 150-167.
- [17] Kyrychko YN, Blyuss KB, Global properties of a delayed SIR model with temporary immunity and nonlinear incidence rate, *Nonlinear analysis: Real World Applications*, 6(3) (2005): 495-507.
- [18] Liu WM, Hethcote HW, Levin SA, Dynamical behavior of epidemiological models with nonlinear incidence rates, *Journal of Mathematical Biology*, 25(4) (1987): 359-380.

- [19] Liu WM, Levin SA, Iwasa Y, Influence of nonlinear incidence rates upon the behavior of SIRS epidemiological models, *Journal of Mathematical Biology*, 23(2) (1986): 187-204.
- [20] Capasso V, *Mathematical structures of epidemic systems*, Springer Science & Business Media, 97 (2008).
- [21] Korobeinikov A, Maini PK, Non-linear incidence and stability of infectious disease models, *Mathematical Medicine and Biology: a Journal of the IMA*, 22(2) (2005): 113-128.
- [22] Capasso V, Serio G, A generalization of the Kermack-McKendrick deterministic epidemic model, *Mathematical Biosciences*, 42(1-2) (1978): 43-61.
- [23] Gomes MG, Margheri A, Medley GF, Rebelo C, Dynamical behaviour of epidemiological models with sub-optimal immunity and nonlinear incidence, *Journal of Mathematical Biology*, 51(4) (2005): 414-430.
- [24] Zhao Y, Analysis of a Dynamic Model of Host-Parasite Interaction with Delay and Treatment, *Chinese Quarterly Journal of Mathematics*, 28 (2013): 118-128.
- [25] Wang ZW, Wang WD, Mathematical Analysis of Immune Response of HIV-I Including Delay, *Chinese Quarterly Journal of Mathematics*, 1 (2010), 10.
- [26] Zhang XB, Huo HF, Sun XK, Fu Q, The differential susceptibility SIR epidemic model with time delay and pulse vaccination, *Journal of Applied Mathematics and Computing*, 34(1-2) (2010): 287-298.
- [27] Dietz K, Transmission and control of arbovirus diseases. *Epidemiology*, 104 (1975): 104-121.
- [28] Levin SA, Hallam TG, Gross LJ, editors, *Applied mathematical ecology*, Springer Science & Business Media, 18 (2012).
- [29] Wang W, Backward bifurcation of an epidemic model with treatment, *Mathematical Biosciences*, 201(1-2) (2006): 58-71.
- [30] Wang W, Ruan S, Bifurcations in an epidemic model with constant removal rate of the infectives, *Journal of Mathematical Analysis and Applications*, 291(2) (2004): 775-793.
- [31] Hu Z, Ma W, Ruan S, Analysis of SIR epidemic models with nonlinear incidence rate and treatment, *Mathematical Biosciences*, 238(1) (2012): 12-20.

- [32] Tripathi JP, Abbas S, Global dynamics of autonomous and nonautonomous SI epidemic models with nonlinear incidence rate and feedback controls, *Nonlinear Dynamics*, 86(1) (2016): 337-351.
- [33] Xiao D, Ruan S, Global analysis of an epidemic model with nonmonotone incidence rate, *Mathematical Biosciences*, 208(2) (2007): 419-429.
- [34] Derrick WR, Van Den Driessche P, A disease transmission model in a nonconstant population, *Journal of Mathematical Biology*, 31(5) (1993): 495-512.
- [35] Hethcote HW, Levin SA, Periodicity in epidemiological models, In *Applied mathematical ecology*, Springer, Berlin, Heidelberg, (1989): 193-211.
- [36] Hethcote HW, Van den Driessche P, Some epidemiological models with nonlinear incidence, *Journal of Mathematical Biology*, 29(3) (1991): 271-287.
- [37] Yuan S, Li B, Global dynamics of an epidemic model with a ratio-dependent nonlinear incidence rate, *Discrete Dynamics in Nature and Society*, (2009).
- [38] Hethcote H, Zhien M, Shengbing L, Effects of quarantine in six endemic models for infectious diseases, *Mathematical biosciences*, 180(1-2) (2002): 141-160.
- [39] Chen TM, Jamil N, Effectiveness of quarantine in worm epidemics, In *2006 IEEE International Conference on Communications*, 5(2142-2147) (2006).
- [40] Zhang Z, Kundu S, Tripathi JP, Bugalia S, Stability and Hopf bifurcation analysis of an SVEIR epidemic model with vaccination and multiple time delays, *Chaos, Solitons & Fractals*, 131 (2020): 109483.
- [41] Gumel AB, Moghadas SM, A qualitative study of a vaccination model with non-linear incidence, *Applied Mathematics and Computation*, 143(2-3) (2003): 409-419.
- [42] Alexander ME, Moghadas SM, Periodicity in an epidemic model with a generalized non-linear incidence, *Mathematical Biosciences*, 189(1) (2004): 75-96.
- [43] Acedo L, González-Parra G, Arenas AJ, An exact global solution for the classical SIRS epidemic model, *Nonlinear Analysis: Real World Applications*, 11(3) (2010): 1819-1825.
- [44] Feng Z, Thieme HR, Recurrent outbreaks of childhood diseases revisited: the impact of isolation, *Mathematical Biosciences*, 128(1-2) (1995): 93-130.

- [45] Hyman JM, Li J, Modeling the effectiveness of isolation strategies in preventing STD epidemics, *SIAM Journal on Applied Mathematics*, 58(3) (1998): 912-925.
- [46] Kar TK, Batabyal A, Modeling and analysis of an epidemic model with non-monotonic incidence rate under treatment, *Journal of Mathematics Research*, 2(1) (2010): 103.
- [47] Li J, Cui N, Dynamic behavior for an SIRS model with nonlinear incidence rate and treatment, *The Scientific World Journal*, (2013).
- [48] Li MY, Muldowney JS, Global stability for the SEIR model in epidemiology, *Mathematical biosciences*, 125(2) (1995): 155-164.
- [49] Li MY, Muldowney JS, A geometric approach to global-stability problems, *SIAM Journal on Mathematical Analysis*, 27(4) (1996): 1070-1083.
- [50] Fan S, A new extracting formula and a new distinguishing means on the one variable cubic equation, *Journal of Hainan Teachers' College (Natural science)*, 2(2) (1989): 91-98.
- [51] Eigenwillig A, Real root isolation for exact and approximate polynomials using Descartes' rule of signs, (2008).
- [52] Zhou L, Fan M, Dynamics of an SIR epidemic model with limited medical resources revisited, *Nonlinear Analysis: Real World Applications*, 13(1) (2012): 312-324.
- [53] Dubey B, Patra A, Srivastava PK, Dubey US, Modeling and analysis of an SEIR model with different types of nonlinear treatment rates, *Journal of Biological Systems*, 21(03) (2013): 1350023.
- [54] Hu Z, Sheng L, Hui W, Backward bifurcation of an epidemic model with standard incidence rate and treatment rate, *Nonlinear Analysis: Real World Applications*, 9(5) (2008): 2302-2312.
- [55] Li J, Teng Z, Wang G, Zhang L, Hu C, Stability and bifurcation analysis of an SIR epidemic model with logistic growth and saturated treatment, *Chaos, Solitons & Fractals*, 99 (2017): 63-71.
- [56] Perko L, *Differential equations and dynamical systems*, Springer Science & Business Media, 7 (2013).

- [57] Marino S, Hogue IB, Ray CJ, Kirschner DE, A methodology for performing global uncertainty and sensitivity analysis in systems biology, *Journal of Theoretical Biology*, 254(1) (2008): 178-196.
- [58] Tripathi JP, Abbas S, Thakur M, Dynamical analysis of a prey–predator model with Beddington–DeAngelis type function response incorporating a prey refuge, *Nonlinear Dynamics*, 80(1-2) (2015): 177-196.
- [59] Zhang X, Liu X, Backward bifurcation of an epidemic model with saturated treatment function, *Journal of mathematical analysis and applications*, 348(1) (2008): 433-443.
- [60] Gumel AB, Ruan S, Day T, Watmough J, Brauer F, Van den Driessche P, Gabrielson D, Bowman C, Alexander ME, Ardal S, Wu J, Modeling strategies for controlling SARS outbreaks, *Proceedings of the Royal Society of London. Series B: Biological Sciences*, 271(1554) (2004): 2223-2232.
- [61] Greenhalgh D, Griffiths M, Backward bifurcation, equilibrium and stability phenomena in a three-stage extended BRSV epidemic model, *Journal of mathematical biology*, 59(1) (2009): 1.
- [62] De Pinho MD, Maurer H, Zidani H, Optimal control of normalized SIMR models with vaccination and treatment, *Discrete & Continuous Dynamical Systems-B*, 23(1) (2018): 79-99.
- [63] Diekmann O, Heesterbeek JA, Metz JA, On the definition and the computation of the basic reproduction ratio  $R_0$  in models for infectious diseases in heterogeneous populations, *Journal of mathematical biology*, 28(4) (1990): 365-382.
- [64] Hethcote HW, Van Ark JW, Epidemiological models for heterogeneous populations: proportionate mixing, parameter estimation, and immunization programs, *Mathematical Biosciences*, 84(1) (1987): 85-118.
- [65] Chitnis N., Hymanb J. M., Cushingc J. M., Determining Important Parameters in the Spread of Malaria Through the Sensitivity Analysis of a Mathematical Model, *Bulletin of Mathematical Biology*, 70: 1272-1296, 2008.
- [66] Samsuzzoha Md., Singh M., Lucy D., Uncertainty and sensitivity analysis of the basic reproduction number of a vaccinated epidemic model of influenza, *Applied Mathematical Modelling*, 37: 903-915, 2013.